Non-lattice Simulations of Supersymmetric Yang-Mills Theories

Ashutosh Tripathi

A dissertation submitted for the partial fulfilment of BS-MS dual degree in Science

Indian Institute of Science Education and Research (IISER) Mohali

April 2022

Certificate of Examination

This is to certify that the dissertation titled **Non-lattice Simulations of Supersymmetric Yang-Mills Theories** submitted by **Ashutosh Tripathi** (MS17101) for the partial fulfilment of BS- MS Dual Degree programme of the institute, has been examined by the thesis committee duly appointed by the institute. The committee finds the work done by the candidate satisfactory and recommends that the report be accepted.

[Dr. K.P. Yogendran] [Dr. Ambresh Shivaji] [Dr. Anosh Joseph]

(Supervisor)

Dated: Monday 18th April, 2022

Declaration

The work presented in this dissertation has been carried out by me under the guidance of Dr. Anosh Joseph at the Indian Institute of Science Education and Research (IISER) Mohali.

This work has not been submitted in part or in full for a degree, a diploma, or a fellowship to any other university or institute. Whenever contributions of others are involved, every effort is made to indicate this clearly, with due acknowledgement of collaborative research and discussions. This thesis is a bonafide record of original work done by me, and all sources listed within have been detailed in the bibliography.

Ashutosh Tripathi
(Candidate)
Dated: Monday 18th April, 2022

In my capacity as the supervisor of the candidate's project work, I certify that the above statements by the candidate are true to the best of my knowledge.

Dr.Anosh Joseph
(Supervisor)
Dated: Monday 18th April, 2022

Acknowledgements

I express my sincere gratitude to my supervisor, Dr. Anosh Joseph, for his patience, motivation, wise remarks, helpful recommendations, and useful information, all of which have greatly aided me in my research and thesis writing. His vast expertise and extensive experience in lattice field theory enabled me to effectively complete my study. I am grateful to him for taking the time to guide me, answer my questions, correct me during my study, and sharing his workstation with me.

Besides my advisor, I wish to thank the rest of my thesis committee members, Dr. K.P Yogendran and Dr. Ambresh Shivaji, for their insightful comments and encouragement.

I extend my sincere thanks to Mr. Arpith Kumar for giving his valuable time during the discussion sessions and helping me during the simulations. I also extend my sincere thanks to Mr. Piyush Kumar for our collaboration on the fermionic calculations of the SUSY model. I acknowledge IISER Mohali for providing me with the best infrastructure and environment for carrying out this project and supporting me with the institute's Merit-cum Means Fellowship.

I want to thank my batch mates and friends for exciting peer discussions throughout the five years of the course. I am also thankful to the THEP (Theoretical High Energy Physics) group of IISER Mohali for holding seminars and journal club activities. These seminars introduced me to various new research being carried out by people of similar interests.

I would also like to thank and acknowledge my parents and relatives for their love and support throughout the years of my studies. This would not have been possible without them.

List of Figures

List of Tables

Abstract

Lattice simulations of supersymmetric gauge theories is not straightforward. In this thesis, we propose a non-lattice method as an alternative to the conventional lattice approach for studying supersymmetric gauge theories. To gain some insight into this non-lattice approach, we first apply it to the supersymmetric anharmonic oscillator model, which is a non-gauge theory and well-studied with the lattice formalism. We extracted the bosonic and fermionic mass gaps from the exponential decay of two-point correlators and compared the results with those obtained from lattice approach. Our simulations also confirm that the SUSY is preserved for the model.

Then, we simulated the bosonic and supersymmetric (SUSY) matrix quantum mechanics model with four supercharges. We used the Polyakov loop as an order parameter to investigate the phase structure of the models at finite temperatures. Our simulations confirmed that the bosonic case exhibits a confinement-deconfinement phase transition as the temperature changes, but the SUSY model always remains in the deconfined phase. Other observables, such as internal energy and space extent, were also computed in addition to the Polyakov loop. Our plots also agreed well with the high-temperature expansion results.

Contents

Chapter 1

Introduction

The development of lattice gauge theory, along with the advancement of various simulation techniques, has provided us with a powerful non-perturbative method for studying gauge theories such as QCD. However, when attempting to apply the method to *supersymmetric gauge theories*, which are interesting for a variety of reasons, some practical and theoretical challenges arise.

First of all, since the algebra of supersymmetry contains continuous translations, which are broken to discrete ones, it seems unavoidable to break it on a lattice. This can be seen immediately if one recalls the supersymmetry algebra $[Q, \bar{Q}] \propto P_\mu$, where the generators for translation appear on the right hand side. Since the translational symmetry is broken by the lattice regularization, one necessarily breaks supersymmetry. Then, one has to include all the relevant terms allowed by symmetries preserved on the lattice, and fine-tune the coupling constants to arrive at the desired supersymmetric fixed point in the continuum limit. One way to deal with this (see Ref. [Giedt 06] and references therein) is that one can reduce the number of parameters to be fine-tuned (even to zero in some cases) by preserving some part of supersymmetry. In lower dimensions, one can alternatively take the advantage of super-renormalizability, and determine the appropriate counter-terms by perturbative calculations to avoid fine-tuning. These two approaches can be nicely illustrated in one dimension by the example of a supersymmetric anharmonic oscillator.

Supersymmetric gauge theories appear in a variety of ways in the context of string/M-theory. The $(p+1)$-dimensional U(N) super Yang-Mills theory, in particular, gives the low-energy effective theory of a stack of N p-branes. This gave rise to a number of intriguing hypotheses. For example, gauge/gravity duality, states that the strong coupling limit of large-N gauge theories has a dual description in terms of classical supergravity. A different but related con-

jecture asserts that non-perturbative superstring/M-theory formulations can be given by matrix models, which can be obtained by dimensionally reducing ten-dimensional $\mathcal{N} = 1$ U(N) super Yang-Mills theory to $D = 0, 1, 2$ dimensions. The $D = 1$ model [Banks 97], in particular, corresponds to the M-theory. The bosonic version has been studied with Monte Carlo simulations using the lattice formulation [Kawahara 07a] and the continuum quenched Eguchi-Kawai model [Kawahara 05]. However, the next step of including fermionic matrices would be difficult even theoretically due to their Majorana-Weyl nature inherited from ten dimensions. Ref. [Kaplan 05] proposed a lattice approach of discretization, which preserves half of SUSY at the expense of breaking the SO(9) symmetry.

The aim of this thesis is to point out that there exists an extremely simple and elegant method to simulate supersymmetric gauge theories, known as **non-lattice simulations**. (We discuss the case of U(N) gauge group, but extension to more general group must be possible.) This method was proposed by three pioneers (M.H., J.N. and S.T.) in 2007 [Hanada 07]. In particular, it will enable us to study the gauge theory side of the aforementioned duality and also to put M-theory on computer.

Let us first recall that the importance of the lattice formulation lies in its manifest gauge invariance. We will be looking at the one-dimensional (1d) case for which the gauge dynamics is almost trivial. (We assume that the 1d direction is compact. The non-compact case would be easier since the gauge dynamics is completely trivial.) This gives us an opportunity to use a non-lattice formulation. More specifically, we first take the static diagonal gauge. Using the residual large gauge transformation, we can choose a gauge slice such that the diagonal elements of the constant gauge field lie within a minimum interval. Finally we expand the fields into Fourier modes, and keep only the modes up to some cutoff. The crucial point of our method is that the gauge symmetry is completely fixed (up to the global permutation group, which is kept intact) before introducing the cutoff.

Notably, one can extend this approach to 3d and 4d gauge theories [Ishiki 09] by using the idea of large-N reduction [Ishii 08]. In the 4d case, the gauge theory becomes superconformal and the number of supersymmetries enhances from 16 to 32. This superconformal theory is interesting on its own right, but it is also studied intensively in the context of the AdS/CFT correspondence, which is a typical case of the gauge-gravity duality. The non-lattice simulation of the 4d superconformal theory requires no fine-tuning, unlike the previous proposals based on the lattice regularization [Kaplan 05].

1.1 One-dimensional Supersymmetric Yang-Mills Models

The non-lattice method has been proved to be very efficient and useful for studying supersymmetric Yang-Mills (SYM) theories in the strongly coupled regime.

1.1.1 The 4 Supercharge Model

The one-dimensional SYM model with four supercharges can be formally obtained by dimensionally reducing four-dimensional $\mathcal{N} = 1$ U(N) super Yang-Mills theory to one dimension. The action of the model is given by

$$S_E = \frac{1}{g^2}\int_0^\beta dt \;\; \mathrm{Tr}\Big[\frac{1}{2}(D_t X_i)^2 - \frac{1}{4}[X_i, X_j]^2 + \bar{\psi} D_t \psi - \bar{\psi}\sigma_i[X_i, \psi]\Big], \tag{1.1}$$

where $D_t X^i = \partial_t X^i - i\,[\,A(t), X^i(t)\,]$ is the covariant derivative with the gauge field $A(t)$ being an $N \times N$ Hermitian matrix. The bosonic matrices $X^i(t)$ with $i = 1,2,3$, are also $N \times N$ Hermitian matrices, and the fermionic matrices $\psi_\alpha(t)$ and $\bar{\psi}_\alpha(t)$ with $\alpha = 1,2$, are $N \times N$ matrices with complex Grassmann entries. The 2×2 matrices σ_i are the Pauli matrices.

1.1.2 The 16 Supercharge Model

The one-dimensional SYM model with sixteen supercharges can be derived by dimensionally reducing ten-dimensional super Yang-Mills theory to one dimension. The action is given by

$$S_E = \frac{1}{g^2}\int_0^\beta dt \;\; tr\left\{\frac{1}{2}(D_t X_i)^2 - \frac{1}{4}[X_i, X_j]^2 + \frac{1}{2}\psi_\alpha D_t \psi_\alpha - \frac{1}{2}\psi_\alpha(\gamma_i)_{\alpha\beta}[X_i, \psi_\beta]\right\}, \tag{1.2}$$

where $D_t X^i = \partial_t X^i - i[\,A(t), X^i(t)\,]$ represents the covariant derivative with the gauge field $A(t)$ being an $N \times N$ Hermitian matrix. The bosonic matrices $X_i(t)$ $(i = 1,2,\cdots,9)$, come from spatial components of the ten-dimensional gauge field, while the fermionic matrices $\psi_\alpha(t)$ $(\alpha = 1,2,\cdots,16)$, come from a Majorana-Weyl spinor in ten dimensions. The 16×16 matrices γ_μ in Eq. (1.2) act on spinor indices and satisfies the Euclidean Clifford algebra $\{\gamma_i, \gamma_j\} = 2\delta_{ij}$.

In both models, we impose periodic and anti-periodic boundary conditions on the bosons and fermions, respectively. The extent β in the Euclidean time direction then corresponds to the inverse temperature $\beta \equiv \frac{1}{T}$. The parameter g in Eq. (1.1) and (1.2) can always be scaled out by an appropriate rescaling of the matrices and the time coordinate t. We take $g = \frac{1}{\sqrt{N}}$ without loss of generality. Both models can be viewed as a one-dimensional U(N) gauge theory.

1.2 Phase Transition

For a system with a density of states that grows exponentially,

$$\rho(E) \sim e^{\beta_H E} \tag{1.3}$$

there exists an upper limit to the temperature known as the Hagedorn temperature. Above this temperature the partition function diverges [Furuuchi 03]

$$\lim_{T \to T_H^-} \mathrm{Tr}\left(\mathrm{e}^{-\beta \mathrm{H}}\right) \to \infty. \tag{1.4}$$

Above this cutoff temperature T_H, the partition function does not exist. However, it can be made to exist if we keep N large but finite. Performing this breaks the exponential growth in the asymptotic density of states at some large but finite energy value. For temperature greater than T_H, the entropy and energy are dominated by the states at and above the cutoff scale and the free energy jumps from $\mathscr{O}(1)$ to $\mathscr{O}(\mathrm{N}^2)$ [Hadizadeh 05]. Thus

$$\lim_{N\to\infty} \frac{F}{N^2} = 0 \qquad \text{(Confined Phase)}, \tag{1.5}$$

$$\lim_{N\to\infty} \frac{F}{N^2} \neq 0 \qquad \text{(Deconfined Phase)}. \tag{1.6}$$

The transition from the confined phase to deconfined phase is known as confinement-deconfinement phase transition or deconfinement phase transition. In the confined phase, the quantum states of the Hamiltonian should be singlets under the gauge symmetry [Semenoff]. This condition fails as soon as the system reaches the Hagedorn temperature. This type of transition is found in large-N gauge theories, such as weakly coupled Yang-Mills theory and it is also expected to be found in the bosonic part of the above discussed one-dimensional SYM models [Semenoff].

This confinement-deconfinement phase transition in the matrix models is associated with the breakdown of the center symmetry, i.e., $A(t) \to A(t) + k\mathbf{1}$. The order parameter for this symmetry breaking is the Polyakov loop [Polyakov 78]. Polyakov loop is defined as the trace of the holonomy of the gauge field around the finite temperature Euclidean time circle

$$P = \frac{1}{N}\mathrm{Tr}\left(\mathrm{P}(\mathrm{e}^{\mathrm{i}\oint \mathrm{dtA(t)}})\right). \tag{1.7}$$

This operator is gauge invariant as it is a special case of the Wilson line operator. The expectation value of this operator is zero in the confined phase and it jumps to a non-zero value as we cross the phase transition point and enters the deconfined phase. This is simply because the

Polyakov loop is a unitary matrix and its eigenvalues are uniformly distributed on the unit circle in the confined phase and in the deconfined phase the eigenvalues clump towards a single point. We have

$$\langle P \rangle = 0 \qquad \text{(Confined phase)}, \tag{1.8}$$

$$\langle P \rangle \neq 0 \qquad \text{(Deconfined Phase)}. \tag{1.9}$$

We will also use this as an order parameter for our simulations of the four supercharge model.

1.3 One-dimensional SYM (16 Supercharges) and Gauge-gravity Duality

One of the motivations to investigate the 16 supercharge version of the 1d SYM model is its dual relationship with the so-called black 0-brane solution in type IIA supergravity. In order for this duality to be valid, one has to take the 't Hooft large-N limit and the strong coupling limit on the gauge theory side.

Given the dual geometry, Hawking's theory of the black hole thermodynamics talks about various thermodynamic relations such as

$$\frac{1}{N^2}\left(\frac{E}{\lambda^{1/3}}\right) = c\left(\frac{T}{\lambda^{1/3}}\right)^{14/5}, \qquad c = \frac{9}{14}\left\{4^{13}15^2\left(\frac{\pi}{7}\right)^{14}\right\}^{1/5} \approx 7.41. \tag{1.10}$$

In the large-N limit, at low T, gauge-gravity duality predicts that this should be reproduced by 1d SYM [Itzhaki 98]. The importance of this prediction is that, if it is true, it explains the microscopic origin of the black hole thermodynamics, meaning that the 1d SYM provides the quantum description of the states inside the black hole.

As another prediction from the gauge-gravity duality, let us consider the Wilson loop, which winds around the temporal direction once, like the Polyakov line. However, unlike the usual Polyakov line, we consider the one involving the adjoint scalar as

$$W \equiv \frac{1}{N}\mathrm{Tr}\mathscr{P}\exp\left[\mathrm{i}\int_0^\beta \mathrm{dt}\{\mathrm{A(t)} + \mathrm{in_i X_i(t)}\}\right], \tag{1.11}$$

where n_i is a unit vector in nine dimensions, which can be chosen arbitrarily due to the SO(9) invariance.

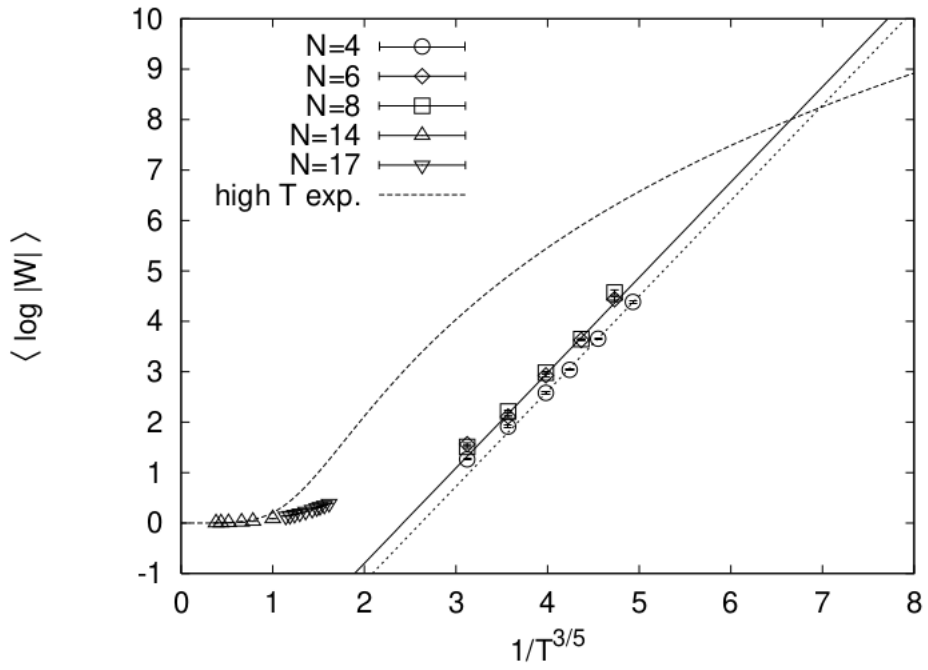

Figure 1.1: Wilson loop against $T^{-3/5}$.

For the model Eq. (1.2), the logarithm of the Wilson loop is given by

$$\ln W = \frac{\beta R_{Sch}}{2\pi\alpha'} = \kappa \left(\frac{T}{\lambda^{1/3}}\right)^{-3/5} \tag{1.12}$$

where R_{Sch} is the Schwarzschild radius of the dual black hole geometry and

$$\kappa = \frac{1}{2\pi}\left\{\frac{16\sqrt{15}\pi^{7/2}}{7}\right\}^{2/5} \approx 1.89. \tag{1.13}$$

Figure 1.1 is a plot of the log of the Wilson loop Eq. (1.11) against $T^{-3/5}$.

At low temperature, the data points are expected to fit nicely to a straight line with a slope 1.89 in precise agreement with Eq. (1.13). The Wilson loop observable helps in extracting the information of dual geometry such as Schwarzschild radius. It also confirms directly the fuzz-ball picture [Mathur 08] of a black hole proposed to solve the information paradox.

Chapter 2

Complex Langevin Dynamics

In this chapter, we will go over the fundamental concepts underlying the complex Langevin dynamics, as well as its recent developments and successes. The primary advantage of this method over traditional Monte Carlo methods is that it does not rely on the action to assign a weight to the field configurations. As we will see, this approach is completely unaffected by the sign problem when it comes to numerical simulations.

2.1 Stochastic Dynamics

The path integral approach, however successful, is not the only way to quantize a quantum field theory. In general, there are various other methods available and, following Ref. [Damgaard 87], we are going to discuss one of the most robust alternatives, namely *stochastic quantizations*. The idea was first introduced by Parisi and Wu [Parisi 81] in 1980 and it consists of considering the Euclidian QFT as an equilibrium limit of a system governed by a stochastic process. The system evolves in an additional time t_L under the effect of some drift force, determined by the system, together with random noise. When the equilibrium is reached, for $t_L \to \infty$, stochastic averages become identical to ordinary Euclidean vacuum expectation values.

The oldest and best known stochastic equation, and the one we are interested in, is the *Langevin equation* [Lemons 97]

$$m\frac{d}{dt}\mathbf{v}(t) = -\alpha\mathbf{v}(t) + \eta(t), \tag{2.1}$$

introduced in 1908 to describe the Brownian motion of a particle of mass m in a fluid with viscosity α that randomly collides with other particles of the fluid with intensity and direction η. The latter is represented by a Gaussian distributed random noise

$$\langle \eta_i(t)\rangle_\eta = 0; \qquad \langle \eta_i(t)\eta_j(t')\rangle_\eta = 2\lambda\,\delta_{ij}\delta(t-t'). \tag{2.2}$$

with a mean of 0 and a variance of 2λ. This old model, however simple and classical, is worth a brief examination in order to gain an understanding of the Langevin stochastic process. Because the Langevin equation Eq. (2.1) is a non-homogeneous first order linear differential equation, it can be solved analytically as the Green's function

$$v_i(t) = \exp\left(-\frac{\alpha}{\mathrm{m}}\mathrm{t}\right)\mathrm{v_i}(0) + \frac{1}{\mathrm{m}}\int_0^{\mathrm{t}} \exp\left(-\frac{\alpha}{\mathrm{m}}(\mathrm{t}-\tau)\right)\eta_{\mathrm{i}}(\tau)\mathrm{d}\tau. \tag{2.3}$$

We notice that the dependence on the initial conditions $v(0)$ is lost exponentially fast with time so that we might as well assume that $v(0) = 0$ without losing any generality. Having an equation for $v(t)$ we want to calculate some physical quantity from it, for example the average kinetic energy of our Brownian particle

$$\begin{aligned}\frac{1}{2}m\langle v^2(t)\rangle &= \frac{1}{2m}\int_0^t d\tau \int_0^t d\tau' \exp\left(-\left(\frac{\alpha}{m}\right)(2t-\tau-\tau')\right)\langle \eta_i(\tau)\eta_j(\tau')\rangle \\ &= \frac{3\lambda}{2\alpha}\left[1 - exp\left(-\frac{2\alpha}{m}t\right)\right].\end{aligned} \tag{2.4}$$

We note that by taking $\lambda = kT\alpha$ the correct value for the average kinetic energy $E = \frac{3}{2}KT$ is recovered for $t \to \infty$. Since eventually we are going to be interested in numerical simulations, it is essential for us to know the behaviour of the probability distribution governing the Langevin stochastic process. Let us set $\lambda = 1$, in this case, the observables will be functions of the velocity $v(t)$

$$\begin{aligned}\langle \mathscr{O}(v(t))\rangle_\eta &\equiv \int D\eta \;\; \exp\left(-\frac{1}{4}\int_0^t \eta^2(\tau)d\tau\right) \;\; \mathscr{O}(v(t)) \\ &= \int dv \;\; \mathscr{O}(v) \;\; P(v,t) \;\equiv\; \langle \mathscr{O}(v(t))\rangle_P,\end{aligned} \tag{2.5}$$

where we used the fact that averages can be computed either over the noise η or over the probability distribution $P(v)$

$$\langle f\rangle_\eta = \langle f\rangle_P. \tag{2.6}$$

Taking the time derivative of Eq. (2.5) and using the Langevin equation (2.1) (with m = α = 1), one gets

$$\left\langle \frac{\partial \mathscr{O}(v)}{\partial v}\frac{dv}{dt}\right\rangle = \left\langle \frac{\partial \mathscr{O}(v)}{\partial v}(-v+\eta)\right\rangle = \int dv \mathscr{O}(v)\frac{\partial P(v,t)}{\partial t}. \tag{2.7}$$

Furthermore, using Eq. (2.5) and integrating by parts, we can write

$$\begin{aligned}\left\langle \frac{\partial \mathscr{O}(v)}{\partial v}\eta \right\rangle &= \int D\eta \left[\frac{\partial}{\partial \eta(t)} \exp\left(-\frac{1}{4}\int_0^t \eta^2(\tau)d\tau\right)\right]\frac{\partial \mathscr{O}(v)}{\partial v} \\ &= 2\left\langle \frac{\partial^2 \mathscr{O}(v)}{\partial v^2}\frac{\partial v}{\partial \eta}\right\rangle = \left\langle \frac{\partial^2 \mathscr{O}(v)}{\partial v^2}\right\rangle,\end{aligned} \tag{2.8}$$

where in the last step we used the expression Eq. (2.3) for $v(t)$

$$\frac{\partial v(t)}{\partial \eta(t)}\int_0^\infty \theta(t-\tau)e^{(}-(t-\tau))\eta_i(\tau)d\tau = \theta(0) = \frac{1}{2}. \tag{2.9}$$

If we adopt the middle point prescription for the Heaviside step function $\theta(t-\tau)$. At this point, we can use Eq. (2.8) and, after applying integration by parts, we can rewrite Eq. (2.7) as

$$\int dv \mathscr{O}(v)\left[\frac{\partial}{\partial v}\left(v+\frac{\partial}{\partial v}\right)\right]P(v,t) = \int dv \mathscr{O}(v)\frac{\partial P(v,t)}{\partial t}. \tag{2.10}$$

This results in the Fokker-Planck equation, which describes the evolution of the probability distribution $P(v,t)$.

$$\frac{\partial P(v,t)}{\partial t} = \frac{\partial}{\partial v}\left(v+\frac{\partial}{\partial v}\right)P(v,t). \tag{2.11}$$

We can notice here that the stationary solution $\frac{\partial}{\partial t}P = 0$ of Eq. (2.11), after requiring the condition $P(v) = P(-v)$, leads to the Boltzmann distribution for the particle in equilibrium with the system

$$P^{eq} \sim \exp\left(-\frac{v^2}{2}\right). \tag{2.12}$$

The Fokker-Planck equation plays a crucial role in the numerical application of the Langevin dynamics in the case of a complex field theory.

2.2 Stochastic Quantization of a Field Theory

The idea behind stochastic quantization is to formulate the equivalent of the Langevin equation, Eq. (2.1) for a field theory in such a way that the associated Fokker-Planck distribution may have the Euclidian Boltzmann distribution $\exp(-S_E)$ as the unique stationary solution.

The first step is the introduction of an additional fictitious time t_L in which the stochastic sys-

tems evolves

$$\phi(x_0,\cdots,x_n) \to \phi(x_0,\cdots,x_n,t_L). \tag{2.13}$$

From now on we are going to call the Langevin time t_L just t, having in mind it is different from the Euclidian time x_0. The second requirement is that the evolution of fields be described by the Langevin stochastic equation

$$\frac{\partial}{\partial t}\phi(x,t) = -\frac{\delta S}{\delta\phi(x,t)} + \eta(x,t), \tag{2.14}$$

where S is the Euclidian action of the field theory, which also depends on the Langevin time

$$S = \int dt\, d^n x\, \mathscr{L}\left(\phi(x,t), \frac{\partial}{\partial t}\phi(x,t)\right) \tag{2.15}$$

and $\eta(x,t)$ is the same Gaussian white noise

$$\langle\eta(x,t)\rangle = 0; \qquad \langle\eta(x,t)\eta(x',t')\rangle = 2\delta^n(x-x')\delta(t-t'). \tag{2.16}$$

In the same way as in the classical case, Eq. (2.14) is associated with a probability distribution function $P(\phi,t)$ for the fields at the Langevin time t

$$\langle\phi(x_1,t),\cdots,\phi(x_n,t)\rangle_\eta = \int D\phi P(\phi,t)\phi(x_1)\cdots\phi(x_n), \tag{2.17}$$

which satisfies the Fokker-Planck equation, corresponding to Eq. (2.11), generalized for the field theory

$$\frac{\partial P(\phi,t)}{\partial t} = \int d^n x \frac{\delta}{\delta\phi(x,t)}\left(\frac{\delta}{S}\delta\phi(x,t) + \frac{\partial}{\partial\phi(x,t)}\right)P(\phi,t). \tag{2.18}$$

As a final remark we would like to show that the Eq. (2.18) leads $P(\phi,t)$ to converge to the Euclidian Boltzmann weight of the standard path integral quantization exponentially fast with Langevin time. Let us consider, for simplicity, one degree of freedom x. The partition function of this system reads

$$Z = \int dx e^{-S(x)} \tag{2.19}$$

and the corresponding Langevin equation is

$$\frac{dx}{dt} = -\partial_x S(x) + \eta. \tag{2.20}$$

The time evolution of the associated probability distribution function $P(x)$

$$\langle O(x))\rangle = \int dx\, O(x)P(x;t) \tag{2.21}$$

which is determined by the Fokker-Planck equation

$$\partial_t P(x,t) = \partial_x[\partial_x + \partial_x S(x)]P(x,t), \tag{2.22}$$

whose stationary point is easily found to be $P(x) \sim e^{-S(x)}$. Moreover, we can rewrite Eq. (2.22) upon the transformation

$$P(x,t) = \psi(x,t)e^{-\frac{1}{2}S(x)}, \tag{2.23}$$

in the form of Schrödinger like equation

$$\dot{\psi}(x,t) = -H_{FP}\psi(x,t) \tag{2.24}$$

where

$$H_{FP} = \left(-\partial_x + \frac{1}{2}S'(x)\right)\left(\partial_x + \frac{1}{2}S'(x)\right). \tag{2.25}$$

The operator Eq. (2.25) is self-adjoint and, if $|\lim_{x\to\infty} S'(x) \to \infty|$, the spectrum of its eigenvalues is non-negative and discrete

$$H\psi_n = E_n\psi_n, \tag{2.26}$$

with the ground state $\psi_0 \sim e^{-S(x)/2}$ annihilating Eq. (2.25). Therefore we can rewrite $\psi(x,t)$ on the base of the eigenvectors of H_{FP}

$$\psi(x,t) = c_0 e^{-\frac{S(x)}{2}} + \sum_n c_n \psi_n(x) e^{-E_n t} \to c_0 e^{-\frac{S(x)}{2}} \tag{2.27}$$

and the correct distribution $P(x) \sim e^{-S(x)}$ is reached exponentially fast.

2.3 Complex Langevin Dynamics

We already discussed how a complex weight prevents the application of standard Monte Carlo methods. On the other hand, stochastic processes do not rely on importance sampling, which makes them good candidates to deal with the sign problem. In this section we shall see how Langevin dynamics can be generalized to the case of complex actions $S(x)$, examining in detail the careful steps that make this method successful.

$$\dot{x} = -S'(x) + \eta(t) \tag{2.28}$$

and, consequently, to the FP equation

$$\partial_t \rho(x,t) = L_0^T \rho(x,t), \tag{2.29}$$

where L_0^T is the usual Fokker-Planck operator $L_0^T = \partial_x(\partial_x + \partial_x S_c(x))$ that now is complex. Eq. (2.29) is expected to have the desired complex weight

$$\rho(x) \sim e^{-S(x)} \tag{2.30}$$

as a stationary solution. However, being complex-valued, $\rho(x)$ is not suitable to be regarded as a probability distribution function (PDF) as in Eq. (2.21). Furthermore, the associated FP Hamiltonian $H_{FP}(z)$, the complex equivalent of Eq. (2.25), is not self-adjoint anymore, so that a proof of exponentially fast convergence to the unique solution cannot be provided. The way to proceed then [Aarts 11b, Aarts 13a], is to consider the real and imaginary parts of the complexified variables $z \to x + iy$ as new and independent degrees of freedom

$$\begin{aligned} \dot{x} &= K_x + \sqrt{N_R}\eta_R, \\ \dot{y} &= K_y + \sqrt{N_I}\eta_I, \end{aligned} \tag{2.31}$$

with the two drifts

$$K_x = -\mathrm{Re}\partial_z S(z), \qquad K_y = -\mathrm{Im}\partial_z S(z). \tag{2.32}$$

The correlators between the noises η_R and η_I derive from the original prescription Eq. (2.2) on the complex noise $\eta = \eta_R + i\eta_I$ and read

$$\begin{aligned} \langle \eta_R(t)\eta_R(t')\rangle &= 2N_R\delta(t-t'), \\ \langle \eta_I(t)\eta_I(t')\rangle &= 2N_I\delta(t-t'), \\ \langle \eta_R(t)\eta_I(t')\rangle &= 0, \end{aligned} \tag{2.33}$$

where $N_R - N_I = 1$ and $\mathrm{N_I} \geq 0$. The complexification of the Fokker-Planck equation

$$\dot{P}(z,t) = \partial_z(N_R\partial_z - K_z)P(z,t) \tag{2.34}$$

can be written, for *holomorphic* observables, in terms of the two independent variables $x(t)$ and $y(t)$ in Eq. (2.31)

$$\dot{P}(x,y,t) = [\partial_x(N_R\partial_x - K_x) + \partial_y(N_I\partial_y - K_y)]P(x,y,t) \tag{2.35}$$

and has the form of a continuity equation with the probability density $P(x,y;t)$ being the charge

$$\dot{P}(x,y,t) = \partial_x J_x + \partial_y J_y, \tag{2.36}$$

and

$$J_x = (N_R\partial_x - K_x)P, \quad J_y = (N_I\partial_y - K_y)P, \tag{2.37}$$

being the currents. Equation (2.35) generates a real PDF for the holomorphic observables

$$\langle\mathscr{O}\rangle_{P(t)} = \int dx\,dy\;\; P(x,y,t)O(x+iy), \tag{2.38}$$

which is, in fact, the main idea of complex Langevin (CL) dynamics, i.e., to reformulate a d-dimensional complex system into a $2d$-dimensional real one. One requirement is to consider the holomorphic continuations of the observables $\langle\mathscr{O}(x)\rangle \to \langle\mathscr{O}(z)\rangle = \langle\mathscr{O}(x+iy)\rangle$. In this sense neither the quantity $\langle\mathscr{O}(x)\rangle$ nor $\langle\mathscr{O}(y)\rangle$ have, by themselves, any meaning in the complexified space.

The reason why complex Langevin dynamics was not largely employed immediately after its introduction in the 80's is that Eq. (2.35), even keeping the same form of the real case, is much harder to solve or to be proved convergent to the appropriate stationary distribution $\rho(x) \sim e^{-S(x)}$ [Klauder 85a, Gausterer 88, Ambjorn 86]. On top of that, unstable solutions of Eq. (2.32) can be found in the complex plane and that was believed to inevitably spoil the dynamics when solved numerically. These two problems have been more recently addressed, allowing CL to become one of the most acknowledged methods when it comes to system affected by the sign problem. The issue of instabilities on the lattice was the first to be successfully and consistently solved [Aarts 10a]. The discretized CL equations for the field ϕ are

$$\begin{aligned}\phi_x^R(n+1) &= \phi_x^R(n) - \varepsilon\ \mathrm{Re}(S'(x_n,y_n)) + \sqrt{\varepsilon}\eta_x^R(n),\\ \phi_x^I(n+1) &= \phi_x^I(n) - \varepsilon\ \mathrm{Im}(S'(x_n,y_n)) + \sqrt{\varepsilon}\eta_x^I(n),\end{aligned} \tag{2.39}$$

where ε is the discrete Langevin time step and x labels the sites of the lattice. When the system is brought near an unstable trajectory $\tau(\phi_R,\phi_I)$, the drifts $K^R(\tau)$ and $K^I(\tau)$ can potentially lead the fields to infinity, in a finite Langevin time $t_L = \varepsilon n$. It turns out that careful integration in the form of adaptive step-size ε_n along those trajectories is enough to completely remove the problem. The idea is to keep the product $\varepsilon_n K$ constant, where $K = f(\sqrt{K_R^2 + K_I^2})$ is a function of the drift to be chosen optimally depending on the system, in order to greatly reduce the step-size ε_n along the unstable trajectories and allow the real component of the random noise η^R to kick the system away from such trajectories. For this purpose, the imaginary component of the random noise η^I is, in general, counter-productive so that is usually preferable to get rid of it. This is in perfect accord with the prescriptions Eq. (2.33) and corresponds to the choice of parameters $N_I = 0$ and $\mathrm{N_R} = 1$.

The problem of convergence of CL is much more complicated to address. Although no definitive solution has been found yet, fundamental progress has been made to fully understand this issue. In particular proofs of convergence have been found to infer, from the distribution of the observables, whether the CL is expected to converge to the right result or not [Aarts 10b, Aarts 11b, Aarts 11a, Aarts 13c, Aarts 13b].

2.4 Problems with Complex Langevin Method

There are a number of problems associated with complex Langevin dynamics, see e.g. Refs. [Klauder 85b]. These can roughly be divided under two headings: instabilities and convergence. The first problem concerns the appearance of instabilities when solving the discretized Langevin equations numerically. Sometimes, but not always, this can be controlled by choosing a small enough step-size. The second problem pertains to convergence. In some cases complex Langevin simulations appear to converge but not to the correct answer.

2.4.1 Adaptive Step-size

The method of adaptive step-size has been proved efficient in dealing with the instabilities associated with the CLM.

Consider a real scalar field ϕ with the Langevin equation of motion

$$\frac{\partial \phi}{\partial \tau} = -\frac{\partial S}{\partial \phi} + \eta. \tag{2.40}$$

Here τ is the supplementary Langevin time, $-\frac{\partial S}{\partial \phi}$ is the drift term derived from the action S, and η is a Gaussian noise. The fundamental assertion of stochastic quantisation is that in the infinite (Langevin) time limit, noise averages of observables become equal to quantum expectation values, defined via the standard functional integral

$$\langle O(\phi)\rangle_S = \frac{\langle O(\phi) e^{-iS_I(\phi)}\rangle_{S_R}}{\langle e^{-iS_I(\phi)}\rangle_{S_R}}, \tag{2.41}$$

where the brackets on the left denote a noise average.

If the action is complex the drift term becomes complex and so the field acquires an imaginary part (even if initially real). One must therefore complexify all fields, $\phi \to \phi_R + i\,\phi_I$. The

Langevin equation then becomes

$$\frac{\partial \phi^R}{\partial \tau} = K^R + \eta, \qquad K^R = -\mathrm{Re}\frac{\partial \mathrm{S}}{\partial \phi}|_{\phi \to \phi_\mathrm{R} + \mathrm{i}\ \phi_\mathrm{I}}, \tag{2.42}$$

$$\frac{\partial \phi^I}{\partial \tau} = K^I, \qquad K^I = -\mathrm{Im}\frac{\partial \mathrm{S}}{\partial \phi}|_{\phi \to \phi_\mathrm{R} + \mathrm{i}\ \phi_\mathrm{I}}. \tag{2.43}$$

Here we restricted ourselves to a real noise. The complexification changes the dynamics substantially. Suppose that before complexification ϕ is a variable with a compact domain, e.g. $-\pi < \phi \leq \pi$. After complexification, the domain is non-compact since $-\infty < \phi^I < \infty$. Moreover, there will be unstable directions along which $\phi_I \to \pm\infty$. This is best seen in classical flow diagrams, in which the drift terms are plotted as a function of the degrees of freedom ϕ_R, ϕ_I. In Fig. 2.1 we show an example of a classical flow diagram in the XY model at finite chemical potential.

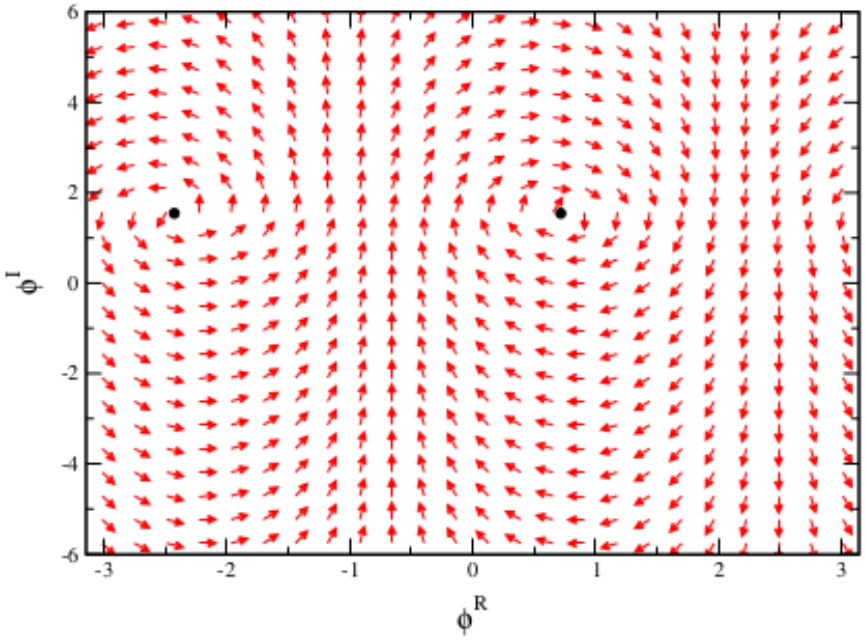

Figure 2.1: Example of a classical flow diagram in the XY model at nonzero chemical potential ($\mu = 2$). The arrows denote the normalized drift terms (K_R, K_I) at (ϕ_R, ϕ_I). The dots are classical fixed points.

The arrows denote the drift terms (K^R, K^I) at (ϕ^R, ϕ^I). The length of the arrows is normalized for clarity. In this case there are unstable directions at $\phi^R \sim -0.7$ and $\phi^\mathrm{R} \sim 2.4$. The black dots denote classical fixed points where the drift terms vanish. Generally speaking, the forces are larger when one is further away from the fixed points. In absence of the noise, one finds generically that configurations reach infinity in a finite time, since the forces grow exponentially for large imaginary field values.

When a Langevin trajectory makes a large excursion into imaginary directions, for instance, by coming close to an unstable direction, sufficient care in the numerical integration of the Langevin equations is mandatory. In some cases it suffices to employ a small step-size ε, after discretizing Langevin time as $\tau = n\varepsilon$. However, this does not solve instabilities in all situations. Moreover, a small step-size will result in a slow evolution, requiring many updates to explore configuration space. To cure both problems, we introduce an adaptive step-size, ε_n, in the discretized Langevin equations

$$\phi_x^R(n+1) = \phi_x^R(n) + \varepsilon_n \, K_x^R(n) + \sqrt{\varepsilon_n}\eta_x(n), \tag{2.44}$$

$$\phi_x^I(n+1) = \phi_x^I(n) + \varepsilon \, K_x^I(n), \tag{2.45}$$

where the noise satisfies

$$\langle \eta_x(n) \rangle_\eta = 0; \qquad \langle \eta_x(n)\eta_{x'}(n') \rangle_\eta = 2\delta_{xx'}\delta_{nn'}. \tag{2.46}$$

The magnitude of the step-size is determined by controlling the distance a single update makes in the configuration space. Here we present two specific algorithms to do this. In the first formulation, we monitor, at each discrete Langevin time n, the quantity

$$K_n^{max} = max|K_x(n)| = max\sqrt{K_x^{R^2}(n) + K_x^{I^2}(n)}. \tag{2.47}$$

We then place an upper bound on the product εK^{max} and define the step-size ε_n as

$$\varepsilon_n = \bar{\varepsilon}\frac{\langle K^{max} \rangle}{K_n^{max}}. \tag{2.48}$$

Here $\bar{\varepsilon}$ is the desired average step-size (which can be controlled) and the expectation value of the maximum drift term $\langle K^{max} \rangle$ is either precomputed, or computed during the thermalisation phase (with an initial guess). In this way, the step-size is completely local in Langevin time and becomes smaller when the drift term is large (e.g. close to an instability) and larger when it is safe to do so. In the second formulation, we keep εK^{max} within a factor p relative to a reference value K. That is,

$$\frac{1}{p}\mathscr{K} \leq \varepsilon K^{max} \leq p\mathscr{K}. \tag{2.49}$$

If this range is exceeded the step-size is increased/reduced by the factor p. This is iterated several times, if necessary. Both p and K have to be chosen beforehand, but this does not require fine tuning as long as clearly inadequate regions are avoided.

2.4.2 Correct Convergence Criteria - Validity of CLM

When one applies CLM to the calculation of expectation values of observables with a complex weight, one necessarily has to complexify the dynamical variables due to the complex drift term, which is derived from the complex weight. Correspondingly, the drift term and the observables should be extended to holomorphic functions of the complexified variables by analytic continuation. Then by measuring the observables for the complexified variables generated by the Langevin process and calculating their expectation values at sufficiently late times, one can obtain the expectation values of the observables for the original real variables with the complex weight.

For a long time, it has been known that this method does not always work. Typically, the complex Langevin process achieves thermal equilibrium without issue, but the results for the expectation values are simply incorrect in some cases. It was discovered that there is a subtlety in the integration by parts used in translating the time evolution of the probability distribution of the complexified variables into that of the observables. The probability distribution of the complexified variables must exhibit appropriate asymptotic behaviour for the integration by parts to be valid.

By now, the following two conditions are relevant in applying the CLM to finite density QCD or any other theory which suffers from sign problem.

- The probability distribution should be suppressed strongly enough when the complexified variables take large values. Typically, this becomes a problem when the complexified variables make long excursions in the imaginary directions during the Langevin simulation.
- The drift term can have singularities while it is otherwise a holomorphic function of the complexified variables. In that case, the probability distribution should be suppressed strongly enough near the singularities.

The crucial point for the success of the CLM turns out to be extremely simple. The probability of the drift term should be suppressed exponentially at large magnitude.

Chapter 3

Supersymmetric Anharmonic Oscillator

In this chapter, we are going to simulate the supersymmetric anharmonic oscillator model. This model is a non-gauge supersymmetric theory and is well studied with the lattice formulation. To gain some insights into the non-lattice approach and to check the validity of simulations, this model would be an excellent starting point. In Ref. [Bergner 08], the same model has been studied on the lattice using various methods. As far as non-gauge theories are concerned, this approach is almost equivalent to the method with the non-local SLAC derivative [Drell 76]. In the lattice case, the only difference is the identification of the modes at the boundary of the Brillouin zone. As a consequence, our results shown in Fig. 3.1 agree with the corresponding results in Ref. [Bergner 08].

3.1 Model and Non-lattice Regularization

The Euclidean action for the model is

$$S = \int_0^\beta dt \, \left[\frac{1}{2}(\partial_t \phi)^2 + h'(\phi)^2 + \bar{\psi}(\partial_t + h''(\phi))\Psi \right], \tag{3.1}$$

where ϕ is a real scalar field, and ψ is a one-component Dirac field, both in 1d, obeying periodic boundary conditions [$\phi(t+\beta) = \phi(t)$ and $\psi(t+\beta) = \psi(t)$]. This model is supersymmetric for arbitrary function $h(\phi)$, but here we take $h(\phi) = \frac{1}{2}m\phi^2 + \frac{1}{4}g\phi^4$.

For regularization purpose, we make a Fourier expansion

$$\phi(t) = \sum_{n=-\Lambda}^{\Lambda} \tilde{\phi}_n e^{in\omega t} \;\; ; \;\; \text{where} \;\; \omega = \frac{2\pi}{\beta} \tag{3.2}$$

and similarly for the fermionic fields, where n takes integer values, and Λ is the UV cutoff. In

terms of the Fourier modes, the action can be written as $S = S_B + S_F$, where

$$S_B = \beta \left[\frac{1}{2} \sum_{n=-\Lambda}^{\Lambda} (n^2\omega^2 + m^2)\tilde{\phi}_n\tilde{\phi}_{-n} + mg(\tilde{\phi}^4)_0 + \frac{1}{2}g^2(\tilde{\phi}^6)_0 \right] \tag{3.3}$$

and

$$S_F = \sum_{n,m=-\Lambda}^{\Lambda} \tilde{\bar{\psi}}_n M_{n,m} \psi_m. \tag{3.4}$$

Here, $M_{n,m}$ is the fermionic matrix with dimensions $(2\Lambda+1)\times(2\Lambda+1)$. The exact form of the fermionic matrix M depends on the potential $h(\phi)$.

For $h(\phi) = \frac{1}{2}m\phi^2 + \frac{1}{4}g\phi^4$, the form is

$$M_{n,m} = \beta \left\{ (in\omega + m)\delta_{nm} + 3g(\tilde{\phi}^2)_l \delta_{n,m+l} \right\}. \tag{3.5}$$

Here, we have used a shorthand notation

$$\left(f^{(1)} \cdots f^{(p)} \right)_n \equiv \sum_{k_1+\cdots+k_p n} f^1_{(k1)} \cdots f^{(}_{(k_p)} p). \tag{3.6}$$

Integrating out the fermionic part of the action, we obtain an effective action

$$S_{\text{eff}} = S_B - \ln \det M, \tag{3.7}$$

where the fermion determinant $\det M$ is real positive for positive m and g.

3.2 CLM for the Model

We simulate the action Eq. (3.7) using the Complex Langevin Method (CLM). We solve the following discretized version of the Langevin equation. Here l is the Langevin time; it is a fictitious parameter, not the real time dimension [1]

$$\phi_n(l+\varepsilon) = \phi_n(l) - \varepsilon \frac{\delta S_{\text{eff}}}{\delta \phi_{-n}} + \sqrt{\varepsilon}\eta_n(l). \tag{3.8}$$

[1] Here, we take the derivative with respect to $\tilde{\phi}_{-n}$, instead of $\tilde{\phi}_n$. Let us consider the one-complex variable case $S = \frac{1}{2}(x^2) + y^2 = zz^*$, with $\mathrm{x}, \mathrm{y} \in \mathrm{R}$ and $\mathrm{z} = \frac{\mathrm{x}+\mathrm{iy}}{\sqrt{2}}, z^* = \frac{\mathrm{x}-\mathrm{iy}}{\sqrt{2}}$. The derivatives for x, y are $\frac{dx}{dt} = -\frac{dS}{dx} = -x$, $\frac{dy}{dt} = -\frac{dS}{dy} = -y$. Hence, we have $\frac{dz}{dt} = -\frac{(x+iy)}{\sqrt{2}} = -z = -\frac{dS}{dz^*} (\neq -\frac{dS}{dz})$.

Equation (3.8) is the evolution equation followed by each Fourier mode. The white noise function $\eta_n(l)$ in the evolution equation has a Gaussian distribution

$$\propto \exp\left(\frac{-1}{4}\sum_{l}\sum_{-\Lambda}^{\Lambda}|\eta_n(l)|^2\right) = \exp\left[\frac{-1}{4}\sum_{l}\left(\eta_0^2(l)+\sum_{1}^{\Lambda}|2\eta_n(l)|^2\right)\right], \tag{3.9}$$

where, $\eta_0(l) = \sqrt{2}x_0(l)$ and $\eta_{\pm n}(l) = x_n(l) \pm iy_n(l)$, each $x_n(l)$ and$y_n(l)(n = 0,1,2,\cdots,\Lambda)$ obeying the standard normal distribution $N(0,1)$ independently.

The gradient is given by

$$\frac{\partial S_{\text{eff}}}{\partial \tilde{\phi}_n} = \beta\left[(n^2\omega^2+m^2)\tilde{\phi}_{-n}+4mg(\tilde{\phi}^3)_{-n}+3g^2(\tilde{\phi}^5)_{-n}\right] - \text{Tr}\left(\frac{\partial M}{\partial \tilde{\phi}_n}M^{-1}\right). \tag{3.10}$$

Here, "Tr" represents the trace of the $(2\Lambda+1)\times(2\Lambda+1)$ matrix. The trace is evaluated as

$$\begin{aligned}\text{Tr}\left(\frac{\partial M}{\partial \tilde{\phi}_n}M^{-1}\right) &= \left(\frac{\partial M}{\partial \tilde{\phi}_n}\right)_{k_1k_2}M^{-1}_{k_2k_1} = 6\beta g\sum_{k2=-\Lambda}^{\Lambda}\underbrace{\left(\sum_{p=-2\Lambda}^{2\Lambda}(\tilde{\phi})_{p-n}\delta_{k_1,k_2+p}\right)}_{=0 \text{ for } |p-n|>(K-2)\Lambda \text{ or } |k1-p|>\Lambda}M^{-1}_{k_2k_1}\\ &= 6\beta g\underbrace{\sum_{p=-2\Lambda}^{2\Lambda}(\tilde{\phi})_{p-n}M^{-1}_{k1-p,k1}}_{=0 \text{ for } |p-n|>(K-2)\Lambda \text{ or } |k1-p|>\Lambda}.\end{aligned} \tag{3.11}$$

In Appendix A, we have given an alternative method for the estimation of $\text{Tr}\left(\frac{\partial M}{\partial \tilde{\phi}_n}M^{-1}\right)$ term.

3.3 Observable - Measurement of Mass

We extract masses from the exponential decay of the two-point correlators.

3.3.1 Bosonic Mass

The bosonic physical mass m_B can be extracted using the correlation function $G_B(t)$, defined as

$$\begin{aligned} G_B(t) = \langle \phi(0)\phi(t)\rangle &= \left\langle \sum_{m,n=-\Lambda}^{\Lambda} \tilde{\phi}_m \tilde{\phi}_n e^{i\omega nt} \right\rangle \\ &= \langle \tilde{\phi}_0^2\rangle + \sum_{n=1}^{\Lambda} \langle \tilde{\phi}_n \tilde{\phi}_{-n}\rangle (e^{iq\omega t} + e^{-in\omega t}) + \sum_{m+n\neq 0} \langle \tilde{\phi}_m \tilde{\phi}_n\rangle e^{in\omega t} = c_0 e^{-m_B t} + \cdots \\ &= b_0 + \sum_{n=1}^{\Lambda} 2b_n \cos(n\omega t), \end{aligned} \tag{3.12}$$

where $b_0 = \langle \tilde{\phi}_0^2\rangle$ and $b_n = \langle \tilde{\phi}_n \tilde{\phi}_{-n}\rangle$. Equation (3.12) satisfies the following relation

$$-\ln \frac{G_B(t+\Delta t)}{G_B(t)} = -\ln \frac{c_0 e^{-m_b(t+\Delta t)}}{c_0 e^{-m_b t}} = -\ln e^{-m_b(\Delta t)} = m_B(\Delta t). \tag{3.13}$$

Hence the mass is obtained at sufficiently large t, where we witness a plateau, as

$$\begin{aligned} m_B &= -\frac{1}{\Delta t} \ln \frac{G_B(t+\Delta t)}{G_B(t)} = -\frac{1}{\Delta t}(\ln G_B(t+\Delta t) - \ln G_B(t)) \\ &= -\frac{d}{dt} \ln G_B(t) = \frac{\sum_{n=1}^{\Lambda} 2n\omega b_n \sin(n\omega t)}{b_0 + \sum_{n=1}^{\Lambda} 2b_n \cos(n\omega t)}. \end{aligned} \tag{3.14}$$

In order to avoid the problem of sharp cut-off in the summation over Fourier modes, that is the Gibbs phenomenon, we extend the sum over n up to 1000 assuming the asymptotic form of the coefficients b_n as $b_n \sim \frac{d_1}{n^2} + \frac{d_2}{n^4}$ at large n [Hanada 07]. The coefficients $d_1, d2$ can be obtained using results at $n = \Lambda - 1, \Lambda$, that is,

$$\begin{aligned} b_{\Lambda-1} &= \frac{d_1}{(\Lambda-1)^2} + \frac{d_2}{(\Lambda-1)^4} \\ b_{\Lambda} &= \frac{d_1}{(\Lambda)^2} + \frac{d_2}{(\Lambda)^4} \\ \implies d_1 &= \frac{\Lambda^4 b_\Lambda - (\Lambda-1)^4 b_{\Lambda-1}}{2\Lambda - 1} \\ d_2 &= \frac{(\Lambda-1)^4\Lambda^2 b_{\Lambda-1} - (\Lambda-1)^2\Lambda^4 b_\Lambda}{2\Lambda-1}. \end{aligned} \tag{3.15}$$

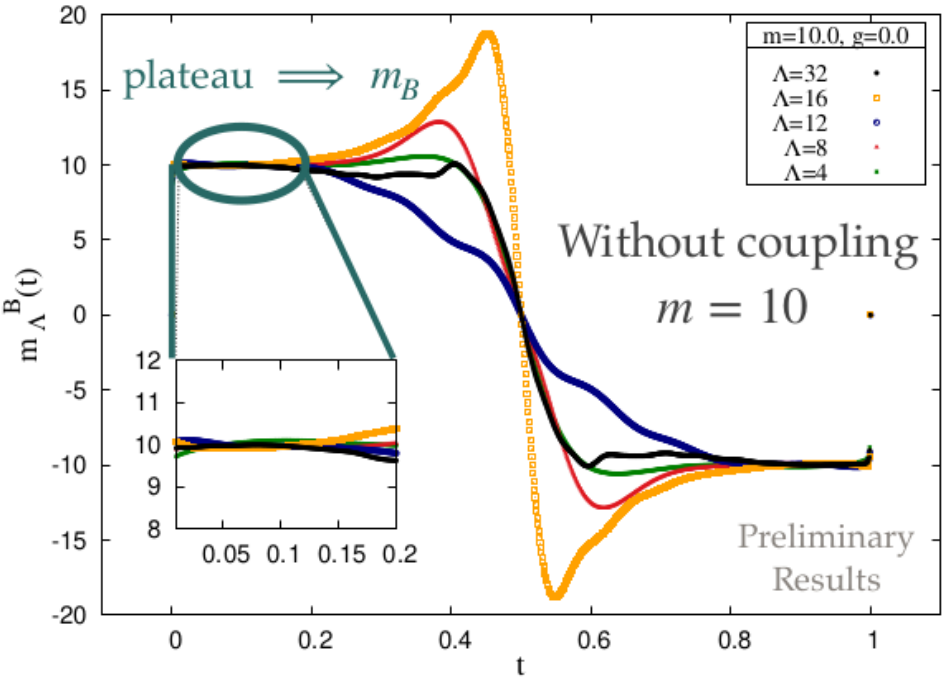

Figure 3.1: Bosonic mass gap coming out as plateau as per Eq. (3.14).

3.3.2 Fermionic Mass

For fermionic mass (m_F), we use fermionic two point correlator, defined as

$$G_F(t) \equiv \langle \psi(0)\bar{\psi}(t)\rangle = \sum_{n=-\Lambda}^{\Lambda} c_n e^{-in\omega t}, \tag{3.16}$$

where we have defined, $c_n \equiv \langle (M^{-1})_{nn}\rangle$. For fermions, it proved convenient to consider, instead of Eq. (3.15), a symmetrized correlator

$$G_F^{(sym)} \equiv \frac{1}{2}\{G_F(t) + G_F(-t)\} = c_0 + \sum_{n=1}^{\Lambda} 2Re(c_n)\cos(n\omega t), \tag{3.17}$$

where we have used the fact $(M_{nk})^* = M_{-n,-k}$. We make an analogous analysis for $\mathrm{Re}(c_n)$ in Eq. (3.16).

Using the above method, we observe clear exponential behaviours, and the physical masses can be extracted from the data using exponential fits.

3.4 Simulation Details and Results

In this section, we will go over the important quantities that are required to monitor reliability of the simulations and compare simulation data to analytical results. The effective dimensionless expansion parameter is $\frac{g}{m^2} = 1$ so this corresponds to a regime of strong coupling.

First, we simulate SUSY harmonic oscillator for physical parameters $m_{\text{phys}} = 10.0$ and $g_{\text{phys}} = 0.0$. Simulations were performed for different Λ keeping the (physical) circle size $\beta = 1$. In Tab. 3.1 we provide the values of the bosonic and fermionic mass gaps. It is clear that $m^B_{phys} \approx m^F_{phys}$ indicating that SUSY is preserved in the model. Fig. 3.2 shows bosonic (red line) and fermionic (blue circle) physical mass gaps versus $\frac{1}{\lambda}$. Black dashed line shows the continuum value of SUSY harmonic oscillator mass gaps for the physical parameters $m_{\text{phys}} = 10.0$ and $g_{\text{phys}} = 0.0$. That is, $m_{exact} = 10$. We see that boson and fermion masses are degenerate within statistical errors, and furthermore, as inverse Fourier cutoff $\frac{1}{\Lambda} \to 0$, the common mass gap approaches the correct continuum value.

Λ	m^B	m^F
2	6.5440	6.4872
4	7.8288	7.7680
6	8.6176	8.7008
8	9.2800	9.2928

Table 3.1: Bosonic and fermionic mass gaps for the SUSY harmonic oscillator with physical parameters $m_{\text{phys}} = 10.0$ and $g_{\text{phys}} = 0.0$. Simulations were performed for $\Lambda = 2, 4, 6, 8$ values. We used adaptive Langevin step size $\Delta\tau \leq 5 \times 10^{-3}$, thermalization steps $N_{\text{therm}} = 10^4$, and generation steps $N_{\text{gen}} = 10^5$. Measurements were taken with a gap of 10 steps.

Now we simulate SUSY anharmonic oscillator for physical parameters $m_{\text{phys}} = 10.0$ and $g_{\text{phys}} = 100.0$. Simulations were again performed for different Λ values keeping the (physical) circle size $\beta = 1$. In Tab. 3.2 we provide the bosonic and fermionic mass gaps. Here also we have $m^B_{\text{phys}} \approx m^F_{\text{phys}}$ indicating that SUSY is preserved in the model. In Fig. 3.3 we show the bosonic and fermionic physical mass gaps versus $\frac{1}{\Lambda}$. Black dashed line shows the continuum value of SUSY anharmonic oscillator mass gaps for the physical parameters $m_{phys} = 10, g_{phys} = 100$ that is $m_{exact} = 16.865$ [Bergner 08]. We see that boson and fermion masses are degenerate within statistical errors, and furthermore as $\frac{1}{\Lambda} \to 0$, the common mass gap approaches the correct continuum value.

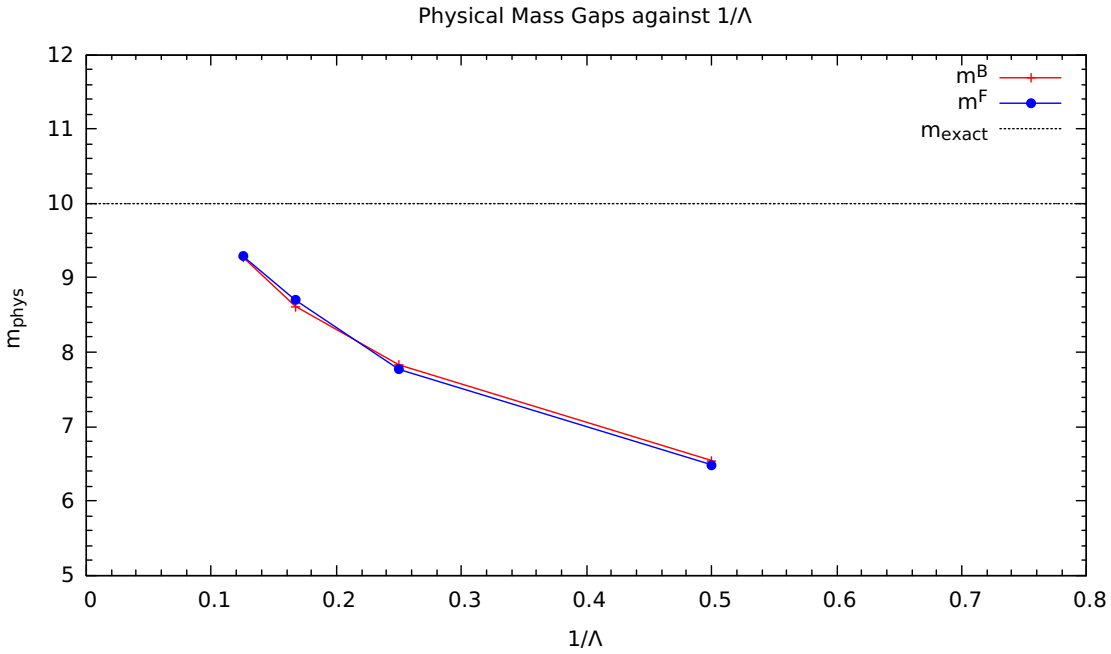

Figure 3.2: Bosonic and fermionic physical mass gaps for SUSY harmonic oscillator against $\frac{1}{\Lambda}$, with physical parameters $m_{\text{phys}} = 10.0$, and $g_{\text{phys}} = 0.0$. The plot is based on the simulation data provided in Tab. 3.1.

Λ	m^B	m^F
2	6.8855	6.8060
4	10.1018	10.0523
6	12.4501	12.7357
8	14.4128	14.6048

Table 3.2: Bosonic and fermionic mass gaps for the SUSY harmonic oscillator with physical parameters $m_{\text{phys}} = 10.0$ and $g_{\text{phys}} = 100.0$. Simulations were performed for $\Lambda = 2, 4, 6, 8$ values. We used adaptive Langevin step size $\Delta\tau \leq 5 \times 10^{-3}$, thermalization steps $N_{\text{therm}} = 10^4$, and generation steps $N_{\text{gen}} = 10^5$. Measurements were taken with a gap of 10 steps.

3.4.1 Reliability of Simulation Results

Thermalization

We started the simulation with a cold start, i.e., all the field configurations were set to zero initially. After that, we updated the field configurations using the Langevin evolution equation.

In Fig. 3.4 we show the Langevin time history of the bosonic action, S_B for $\lambda = 4, 16, 32$. The action for each Λ is oscillating about some value, which shows that the system has been thermalized, and now we can collect the data for our calculation purpose.

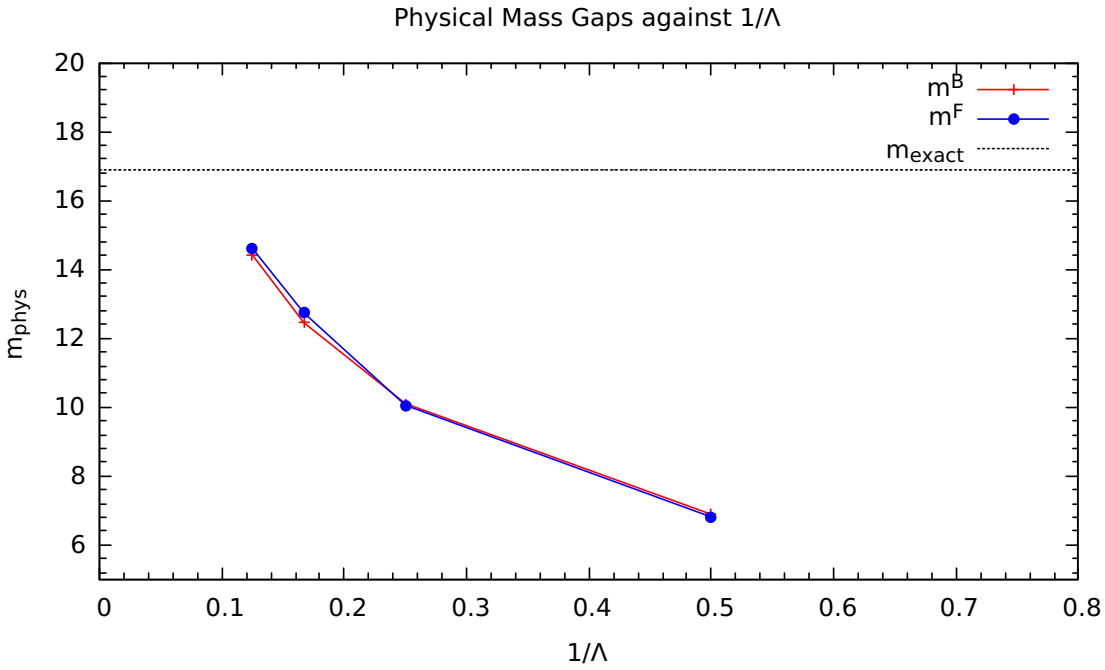

Figure 3.3: Bosonic and fermionic physical mass gaps for SUSY anharmonic oscillator against $\frac{1}{\Lambda}$, with physical parameters $m_{\text{phys}} = 10.0$, and $g_{\text{phys}} = 100.0$. The plot is based on the simulation data provided in Tab. 3.2.

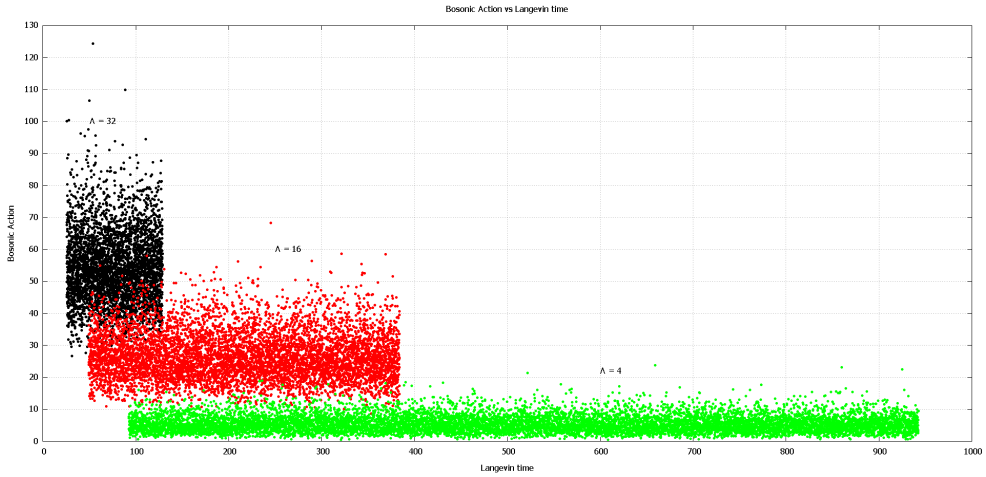

Figure 3.4: Langevin time history of the bosonic action S_B for physical parameters $m_{phys} = 10$ and $g_{phys} = 100$.

Decay of the Drift Terms

Another test to check the correctness of the complex Langevin simulation results, as proposed in Refs. [Nagata 16, Nagata 16], is to look at the probability distribution $P(u)$ of the magnitude

of the drift term u at large values of the drift. We have the magnitude of the mean drift

$$u = \sqrt{\frac{1}{2\Lambda+1}\sum_{n=-\Lambda}^{\Lambda}\left|\frac{\partial S_{eff}}{\partial \tilde{\phi}_{-n}}\right|^2}. \tag{3.18}$$

In Refs. [Nagata 16, Nagata 16] the authors demonstrated, in a few simple models, that the probability of the drift term should be suppressed exponentially at larger magnitudes in order to guarantee the correctness of complex Langevin method. In Fig. 3.5, we show the probability distribution $P(u)$ of the magnitude of the mean drift term u, for different Λ values. It is clear from the plot that the probability of drift is suppressing exponentially. Hence, the simulation results are reliable.

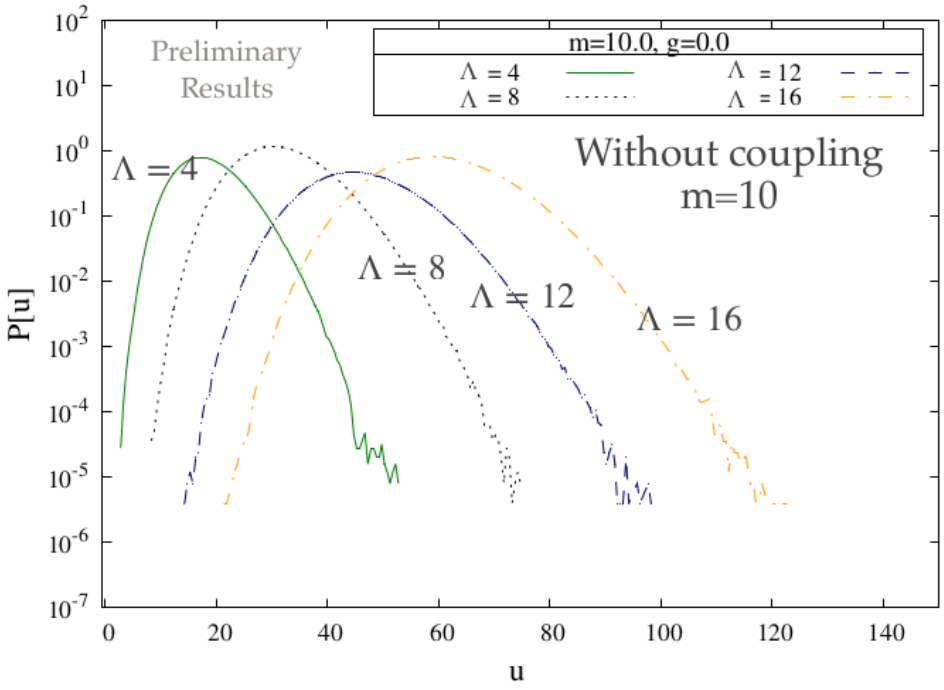

Figure 3.5: Probability of drift plotted for $\Lambda = 4, 8, 12, 16$ at $m = 10$ and $g = 0.0$.

Chapter 4

Bosonic Matrix Quantum Mechanics

In this chapter, we are first going to discuss how to implement non-lattice method in case of one-dimensional gauge theories and then apply this technique to simulate the bosonic matrix quantum mechanics model with four supercharges. Simulations including fermions will be discussed in the next chapter.

4.1 Gauge Symmetries and Gauge Fixing

Let us first discuss a little bit about gauge symmetries and gauge fixing procedures before going to the model.

Gauge symmetry is not a true symmetry, but rather a reflection of a theory's redundant degrees of freedom. The existence of different field configurations that are equivalent is implied by gauge symmetry. For example, consider a U(1) theory with fields A_μ and ψ. The fields transform as

$$\psi \longrightarrow e^{i\alpha(x)}\psi,$$
$$A_\mu \longrightarrow A_\mu + \frac{1}{e}\partial_\mu \alpha(x).$$

Here, the phase of ψ as well as the longitudinal part of A_μ are not physical degrees of freedom. A massless spin-1 representation of the Lorentz group has only two polarizations. A_μ has four components. Thus, to have a Lorentz covariant formulation, we require gauge symmetries to get rid of the extra degrees of freedom.

When quantizing the theory, we should separate the redundant and physical degrees of freedom. We need to make sure only physical modes contribute to observables. This leads to complications in dealing with gauge theories. There are two general approaches:

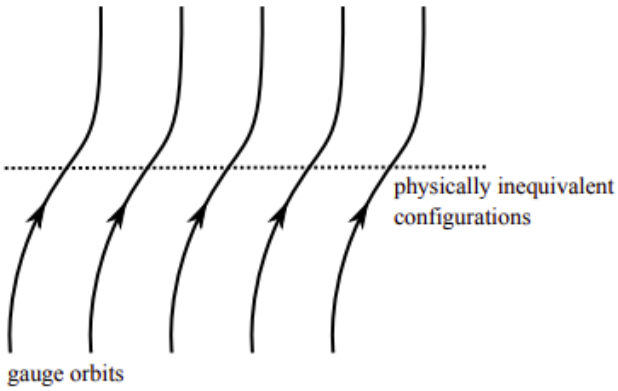

Figure 4.1: Equivalent gauge orbits in configuration space.

1. Isolate the physical degrees of freedom: fix a gauge and quantize the resulting constrained system. This method is used, for example, in axial gauge quantization in quantum electrodynamics.

2. Retain the nonphysical modes, or even introduce additional modes, but make sure that they do not contribute to any physical observables. This method is used, for example, in covariant path integral quantization.

4.1.1 Faddeev-Popov Ghosts

The equivalence principle implies that in the functional integral approach, one must integrate over classes of gauge equivalent fields rather than integrating over all fields.

Let $S(A)$ be the action of our theory, which is a function of gauge field A^a_μ.

The choice of the representatives in the classes of equivalent fields is realized by means of a gauge condition (gauge fixing). For instance,

$$\partial_\mu A^a_\mu = 0. \tag{4.1}$$

This condition defines a plane in the set of all fields, which is intersected by the gauge orbits defined above.

In this context, the difference among Abelian and non-Abelian cases becomes clear. In the Abelian case, we take $\Omega(x) = \exp i\Delta(x)$ and a gauge orbit is defined by

$$A_\mu \longrightarrow A_\mu + \partial_\mu \Lambda, \tag{4.2}$$

which is just a linear shift. Thus all the Abelian orbits intersect the gauge surface at the same angle. In the non-Abelian case, the gauge orbit equations are non-linear and the intersection angle depends on the field parameterizing the orbit. It is clear that this must be taken into account in the functional integral.

More explicitly, in the naive integral

$$\int \exp\{iS(A)\}\prod_x \delta_\mu A_\mu \prod_{x,a} dA^a_\mu, \tag{4.3}$$

where we integrate the Feynman weight exp($i\hbar$action) over all fields, we should introduce a factor taking into account this angle. It is intuitively clear that this factor is a determinant of some operator. The only natural candidate operator for this determinant is the one obtained from an infinitesimal change of the gauge condition. An infinitesimal gauge transformation is defined via the function $\varepsilon(x)$ with values in the Lie algebra G

$$\delta A_\mu = \partial_\mu \varepsilon - [A_\mu, \varepsilon]. \tag{4.4}$$

The corresponding change of the gauge condition is

$$\delta(\partial_\mu A_\mu) = M(A)\varepsilon = \partial^2_\mu \varepsilon - \partial_\mu [A_\mu, \varepsilon]. \tag{4.5}$$

The dependence of $M(A)$ on the field A is due to the second, non-linear, term in Eq. (4.5), which is absent in the Abelian case.

Thus, we can modify the functional integral to

$$\int \exp\{iS(A)\}\prod_x \delta_\mu A_\mu \prod_{x,a} \det M(A)\, dA^a_\mu. \tag{4.6}$$

In the Abelian case, the determinant $\det M$ does not depend on A and gives a constant factor, which does not influence the physical quantities. In the non-Abelian case, this determinant adds to the perturbative expansion some new terms.

Now, let $\Delta(A)$ be given by

$$\Delta(A)^{-1} = \int \prod \delta(\partial_\mu A^\Omega_\mu \prod_x d\Omega). \tag{4.7}$$

This integral is apparently gauge invariant and, on the gauge surface $\partial_\mu A_\mu = 0$, it is equal to

$$\int \prod \delta(M(A)\varepsilon) \prod d\varepsilon = \frac{1}{\det M(A)}. \tag{4.8}$$

4.2 Model and Non-Lattice Discretization

In this section we will discuss the bosonic counterpart of supersymmetric matrix quantum mechanics model with four supercharges. The model can be formally obtained by dimensionally reducing 4d $\mathcal{N} = 1$ U(N) pure Yang-Mills theory to 1 dimension. (The totally reduced model has been studied by Monte Carlo simulation in Ref. [Ambjørn 00]). The Euclidean action of the model is given by

$$S_E = \frac{1}{g^2} \int_0^\beta \mathrm{dt}\ \mathrm{Tr} \left\{ \frac{1}{2} (\mathrm{D_t X_i})^2 - \frac{1}{4} [\mathrm{X_i}, \mathrm{X_j}]^2 \right\}. \tag{4.9}$$

Here, D_t represents the covariant derivative $D_t \equiv \partial_t - i\,[\,A(t),\,.\,]$. The one-dimensional fields $A(t)$ and $X_i(t)$ $(i = 1,2,3)$ are $N \times N$ Hermitian matrices, which can be regarded as the gauge field and three adjoint scalars, respectively. The Euclidean time t has a finite extent β, which corresponds to the inverse temperature $\beta = \frac{1}{T}$, and all the fields obey periodic boundary conditions. A suitable rescaling of the matrices and the time coordinate t can always absorb the parameter g in Eq. (4.9). Therefore, we can set $g = \frac{1}{\sqrt{N}}$ without any loss of generality.

The importance of the lattice formulation lies in its manifest gauge invariance. In the present 1d case, however, the gauge dynamics is almost trivial. (We assume that the 1d direction is compact. The non-compact case would be easier, since the gauge dynamics is completely trivial.) This gives us an opportunity to use a non-lattice formulation.

More specifically, we first take the static diagonal gauge. Using the residual large gauge transformation, we can choose a gauge slice such that the diagonal elements of the constant gauge field lie within a minimum interval. Finally, we expand the fields into Fourier modes, and keep only the modes up to some cutoff. The crucial point of our method is that the gauge symmetry is completely fixed (up to the global permutation group, which is kept intact) before introducing the cutoff.

Let us take a static diagonal gauge

$$A(t) = \frac{1}{\beta} \mathrm{diag}(\alpha_1, \alpha_2, \cdots, \alpha_\mathrm{N}), \tag{4.10}$$

where $\alpha_a (a = 1, 2, \cdots, N)$ can be chosen to lie within the interval $(-\pi, \pi]$ by making a gauge transformation with a non-zero winding number$(k \neq 0)$. In the present case with only adjoint representations, it is more convenient to impose a weaker constraint $\max(\alpha_i) - \min(\alpha_i) < 2\pi$, which respects the center U(1) symmetry $\alpha_i \longrightarrow \alpha_i + \text{const}$.

We have to add to the action a term

$$S_{FP}(\alpha) = -\sum_{a<b} 2\ln|\sin\frac{\alpha_a - \alpha_b}{2}|, \tag{4.11}$$

which appears from the Faddeev-Popov procedure discussed in Eq. (4.1.1), and the integration measure for α_a is taken to be uniform.

$$\begin{aligned} Z &= \int \mathscr{D}A\ \mathscr{D}X\ e^{-S[X,A]} \\ &\propto \int \prod_{a=1}^{N} d\ \alpha_a \prod_{a>b}^{N} |e^{i\alpha_a} - e^{i\alpha_b}|^2\ \mathscr{D}X\ e^{-S[X,A]} \\ &\propto \int \prod_{a=1}^{N} d\alpha_a \prod_{a>b}^{N} sin^2(\frac{\alpha_a - \alpha_b}{2})\ \mathscr{D}X\ e^{-S[X,A]} \\ &\propto \int \prod_{a=1}^{N} d\alpha_a\ \mathscr{D}X\ e^{-S[X,A(\alpha)]-S_{FP}(\alpha)}, \end{aligned} \tag{4.12}$$

where $S_{FP}(\alpha)$ is known as Faddeev-Popov term, and it is given by

$$S_{FP}(\alpha) = -\sum_{a\neq b} \ln\left|\sin\frac{\alpha_a - \alpha_b}{2}\right|. \tag{4.13}$$

The integration measure for α_a is taken to be uniform.

Now, we need to discretize our theory and for that purpose we are using non-lattice method. The whole procedure is mentioned in Ref. [Hanada 07]. We will use the same procedure here also.

We make a Fourier expansion of our matrix fields

$$X_i^{ab}(t) = \sum_{n=-\Lambda}^{\Lambda} \tilde{X}_{in}^{ab} e^{i\omega nt}. \tag{4.14}$$

The kinetic part of the action, Rq. (4.9), transforms as follows

$$\begin{aligned}(D_t X_i)^2 &= (\ \partial_t X_i(t) - i\ [\,A(t),\ X_i(t)]\ )(\ \partial_t X_i(t) - i[A(t),X_i(t)]\ ) \\ &= (\ \partial_t X_i(t)\ )^2 - i\ [\ [A(t),X_i(t)],\partial_t X_i(t)\ ] - [\,A(t),\ X_i(t)\ ]^2. \end{aligned} \tag{4.15}$$

On using transformation Eq. (4.14) in Eq. (4.15), the three terms transforms as follows.

First term-

$$\left(\partial_t X_i^{ab}(t)\right)^2 = \left[\sum_{m=-\Lambda}^{\Lambda} i\omega m\ \ \tilde{X}_{im}^{ab} e^{i\omega m t}\right]\left[\sum_{n=-\Lambda}^{\Lambda} i\omega n\ \ \tilde{X}_{in}^{bc} e^{i\omega n t}\right]. \tag{4.16}$$

Performing integration over time t gives

$$\begin{aligned} N\int_0^\beta \mathrm{dt\ Tr}\left[(\partial_t\ \mathrm{X_i^{ab}(t)})^2\right] &= N\ \mathrm{Tr}\left[\sum_{\mathrm{m,n=-\Lambda}}^{\Lambda} \mathrm{i}\omega\mathrm{m}\ \ \tilde{\mathrm{X}}_{\mathrm{im}}^{\mathrm{ab}}\ \mathrm{i}\omega\mathrm{n}\ \ \tilde{\mathrm{X}}_{\mathrm{in}}^{\mathrm{bc}} \int_0^\beta \mathrm{dt e^{i\omega(m+n)t}}\right] \\ &= -N\ \mathrm{Tr}\left[\sum_{\mathrm{m,n=-\Lambda}}^{\Lambda} (\omega\mathrm{m})(\omega\mathrm{n})\ \tilde{\mathrm{X}}_{\mathrm{im}}^{\mathrm{ab}}\ \tilde{\mathrm{X}}_{\mathrm{in}}^{\mathrm{bc}}\ \frac{2\pi}{\omega}\ \delta(\mathrm{m+n})\right] \\ &= -N\beta\ \mathrm{Tr}\left[\sum_{\mathrm{n=-\Lambda}}^{\Lambda} (-\omega\mathrm{n})(\omega\mathrm{n})\ \tilde{\mathrm{X}}_{\mathrm{i,-n}}^{\mathrm{ab}}\ \tilde{\mathrm{X}}_{\mathrm{in}}^{\mathrm{bc}}\right] \\ &= N\beta\mathrm{Tr}\left[\sum_{\mathrm{n=-\Lambda}}^{\Lambda} (\omega\mathrm{n})^2\ \ \tilde{\mathrm{X}}_{\mathrm{i,-n}}^{\mathrm{ab}}\tilde{\mathrm{X}}_{\mathrm{in}}^{\mathrm{bc}}\right] \\ &= N\beta\left[\sum_{a,b}\ \sum_{n=-\Lambda}^{\Lambda} (\omega n)^2\ \ \tilde{X}_{i,-n}^{ab}\tilde{X}_{in}^{ba}\right]. \end{aligned} \tag{4.17}$$

Last term- - The last term involves square of the commutator $(\ [\,A(t),\ X_i(t)]\ )$. This commutator can also be viewed as

$$\begin{aligned}[A(t),X_i(t)]_{ab} &= \sum_n (A_{an}(X_i)_{nb} - (X_i)_{an}A_{nb}) \\ &= \sum_n \alpha_n\delta_{an}(X_i)_{nb} - (X_i)_{an}\alpha_n\delta_{nb} \\ &= \alpha_a(X_i)_{ab} - (X_i)_{ab}\alpha_b\ =\ (\alpha_a-\alpha_b)(X_i)_{ab}. \end{aligned} \tag{4.18}$$

Performing integration over time t gives

$$
\begin{aligned}
N\int_0^\beta \mathrm{dtTr}\left([\mathrm{A(t)},\mathrm{X_i(t)}]^2\right) &= N\int_0^\beta \mathrm{dtTr}\left([\mathrm{A(t)},\mathrm{X_i(t)}]_{\mathrm{ab}}[\mathrm{A(t)},\mathrm{X_i(t)}]_{\mathrm{bc}}\right) \\
&= N\int_0^\beta \mathrm{dt}\sum_{\mathrm{a,b}}\left((\alpha_{\mathrm{a}}-\alpha_{\mathrm{b}})(\mathrm{X_i})_{\mathrm{ab}}(\alpha_{\mathrm{b}}-\alpha_{\mathrm{a}})(\mathrm{X_i})_{\mathrm{ba}}\right) \\
&= N\sum_{a,b}\left(-(\alpha_a-\alpha_b)^2\left[\sum_{m,n=-\Lambda}^{\Lambda}\tilde{X}^{ab}_{im}\tilde{X}^{ba}_{in}\int_0^\beta \mathrm{dte}^{\mathrm{i}\omega(\mathrm{m+n})\mathrm{t}}\right]\right) \\
&= N\beta\left(\left[\sum_{a,b}\sum_{n=-\Lambda}^{\Lambda}-(\alpha_a-\alpha_b)^2\tilde{X}^{ab}_{i,-n}\tilde{X}^{ba}_{in}\right]\right).
\end{aligned}
\tag{4.19}
$$

Similarly, the middle term in Eq. (4.15) becomes

$$
-i\left[[A(t),X_i(t)],\partial_t X_i(t)\right] = -N\beta\left[\sum_{a,b}\sum_{n=-\Lambda}^{\Lambda}2n\omega\frac{(\alpha_a-\alpha_b)}{\beta}\tilde{X}^{ab}_{i,-n}\tilde{X}^{ba}_{in}\right]. \tag{4.20}
$$

Combining Eqs. (4.17), (4.19), and (4.20) gives the final discretized action

$$
S_{\mathrm{regular}} = N\beta\left[\frac{1}{2}\sum_{n=-\Lambda}^{\Lambda}\left\{n\omega-\frac{\alpha_a-\alpha_b}{\beta}\right\}^2\tilde{X}^{ba}_{i,-n}\tilde{X}^{ab}_{in}-\frac{1}{4}\mathrm{Tr}\left([\mathrm{X_i},\mathrm{X_j}]^2\right)_0\right]. \tag{4.21}
$$

If we also consider the additional term obtained from gauge fixing, the effective action becomes

$$
S_{\mathrm{eff}} = N\beta\left[\frac{1}{2}\sum_{n=-\Lambda}^{\Lambda}\left\{n\omega-\frac{\alpha_a-\alpha_b}{\beta}\right\}^2\tilde{X}^{ba}_{i,-n}\tilde{X}^{ab}_{in}-\frac{1}{4}\mathrm{Tr}\left([\mathrm{X_i},\mathrm{X_j}]^2\right)_0\right]-\sum_{a<b}2\ln\left|\sin\frac{\alpha_{\mathrm{a}}-\alpha_{\mathrm{b}}}{2}\right|. \tag{4.22}
$$

We will use the action Eq. (4.22) for the simulation purpose.

4.3 CLM for Bosonic Model

Langevin dynamics provides us with the stochastic evolution of the dynamical field configuration, in a fictitious time t, governed by the following equation

$$
\frac{d\phi}{dt} = -\frac{\partial S[\phi]}{\partial\phi}+\eta(t). \tag{4.23}
$$

The Langevin evolution equation contains drift term. Here, for our model we will have two kind of drift terms corresponding to two field variables. First are gauge variables α_k, which is a one-dimensional array of size N and other are scalar fields X^i_n, which are $N\times N$ Hermitian matrices.

The drift terms can be calculated using the action Eq. (4.22), and are given by

$$\frac{-\partial S_{eff}}{\partial \alpha_a} = N\left[\sum_{b=1}^{N}\left\{\left(n\omega - \frac{\alpha_a-\alpha_b}{\beta}\right)\right\}\tilde{X}^{ba}_{i,0}\tilde{X}^{ab}_{i,2\Lambda}\right] + \frac{1}{2}\sum_{\substack{b=1\\a\neq b}}^{N}\cot\left(\frac{\alpha_a-\alpha_b}{2}\right), \tag{4.24}$$

$$\frac{-\partial S_{eff}}{\partial X^i_{n,ab}} = -\frac{N\beta}{2}\left[\left(n\omega - \frac{\alpha_a-\alpha_b}{\beta}\right)^2\tilde{X}^i_{-n,ba}\right] + N\beta[X_j,[X_i,X_j]]_{ba}\delta_{n,0}. \tag{4.25}$$

The gradient of the trace of the commutator square term is given by

$$\frac{1}{4}\frac{\partial}{\partial (X_i)_{ba}}\mathrm{Tr}\left([\mathrm{X_i},\mathrm{X_j}]^2\right) = 2\sum_{j=1}^{3}(X_jX_iX_j)_{ab} - \sum_{j=1}^{3}\left[(X_iX_jX_j)_{ab} + (X_jX_jX_i)_{ab}\right]. \tag{4.26}$$

4.4 Observables

The observables that we will be looking at are the Polyakov loop $|P|$, the extent of space R^2, and the internal energy E. The definition and the discretized forms of these observables are given below.

- Polyakov loop $|P|$

$$\langle|P|\rangle \equiv \frac{1}{N}\left\langle\left|\mathscr{P}(e^{i\oint dtA(t)})\right|\right\rangle = \left\langle\left|\frac{Tr(U)}{N}\right|\right\rangle, \tag{4.27}$$

  where the symbol $\mathscr{P}$ exp represents the path-ordered exponential and the unitary matrix U is called the holonomy matrix.

- Extent of space (R^2)

$$\begin{aligned}\langle R^2\rangle &\equiv \left\langle\frac{1}{N\beta}\int_0^\beta \mathrm{dtTr}(\mathrm{X^{i^2}})\right\rangle \\ &= \left\langle\frac{1}{N\beta}\left[\mathrm{Tr}(\mathrm{X^i_0})^2 + \sum_{\mathrm{n}=-\Lambda}^{\Lambda}\mathrm{Tr}(\mathrm{X^i_n})^2\right]\right\rangle \quad \text{(discretized form)}.\end{aligned} \tag{4.28}$$

- Internal energy E

  As a fundamental quantity in thermodynamics, the free energy $F \equiv -\frac{1}{\beta}lnZ(\beta)$ is defined in terms of the partition function

$$Z[\beta] = \int [\mathscr{D}X]_\beta [\mathscr{D}A]_\beta] e^{-S(\beta)}, \tag{4.29}$$

where the suffix of the measure $[.]_\beta$ represents the period of the field to be path-integrated. However, the free energy F cannot be calculated straightforwardly by Monte Carlo simulation because that would require evaluation of the partition function $Z(\beta)$. We therefore study the internal energy defined by

$$E \equiv \frac{d}{d\beta}(\beta F) = -\frac{d}{d\beta} log Z(\beta), \tag{4.30}$$

which has equivalent information as the free energy (given that $F = E$ at $T = 0$). Note also that the internal energy at $T = 0$ provides the ground state energy of the quantum mechanical system. In Appendix B we have derived this formula

$$\frac{1}{N^2}E = \frac{3}{4}\langle F^2 \rangle, \tag{4.31}$$

$$F^2 \equiv \frac{-1}{N}\int_0^\beta \mathrm{dtTr}([\mathrm{X}^\mathrm{i}, \mathrm{X}^\mathrm{j}]^2), \tag{4.32}$$

where the symbol $\langle . \rangle$ represents the expectation value with respect to $Z(\beta)$. This formula enables us to calculate the internal energy E directly by Monte Carlo or real Langevin simulations.

The discretized form used for the simulations is given by

$$\begin{aligned}\left\langle \frac{E}{N^2} \right\rangle &\equiv \left\langle \frac{-3}{4N\beta}\int_0^\beta \mathrm{dtTr}([\mathrm{X}^\mathrm{i}, \mathrm{X}^\mathrm{j}]^2) \right\rangle \\ &= \left\langle \frac{-3}{4N\beta}\sum_{n=-\Lambda}^{\Lambda} \mathrm{Tr}([\mathrm{X}^\mathrm{i}_\mathrm{n}, \mathrm{X}^\mathrm{j}_\mathrm{n}]^2) \right\rangle.\end{aligned} \tag{4.33}$$

4.5 Simulation Details and Results

In the simulations each variable and parameter have been measured in units of 't Hooft coupling λ_0. The physical properties of the system depend only on the dimensionless effective coupling constant given by

$$\lambda_{eff} = \frac{\lambda}{T^3}. \tag{4.34}$$

In what follows we set $\lambda = 1$ without loss of generality. One can confirm this statement by rescaling the fields and the coordinate t appropriately so that all the λ and T dependence appears in the combination of Eq. (4.34). Thus, every variable and parameter appearing in Eq. (4.22) are dimensionless. We simulated the model for parameter values $N = 2$ and $\Lambda = 2$. We

run the simulations for 15 different temperature values. We used adaptive Langevin step-size ($\Delta\tau \leq 5 \times 10^{-3}$), thermalization steps $N_{therm} = 10^4$, and generation steps $N_{gen} = 10^5$. Measurements were taken with a gap of 10 steps.

The results are provided below. Our results are in excellent agreement with the results given in Ref. [Hanada 07]

Polyakov Loop $|P|$

It is known that the bosonic matrix quantum mechanics undergoes a phase transition [Aharon 04, Janik 00] at some critical temperature, which can be interpreted as the Hagedorn transition in string theory. This transition is associated with the spontaneous breakdown of the U(1) symmetry and therefore it is analogous to the confinement/deconfinement transition in ordinary gauge theories.

$$A(t) \longrightarrow A(t) + \alpha \mathbf{1}. \tag{4.35}$$

The Polyakov loop $|P|$ acts as an order parameter for this phase transition. Fig. 4.2 shows the plot of Polyakov loop against temperature obtained from the simulation. The black and red curves show the leading and next-to-leading terms of the high temperature expansion calculations given in Ref. [Kawahara 07b]. The system remains in the confined phase for small temperature, and after crossing the critical temperature T_c, the system moves to the deconfined phase. In the limit $N \to \infty$ the plot will be given by the Heaviside step function with the discontinuity at the critical temperature T_c. So for a finite system we fit our plot of the Polyakov loop with a suitable function that in the limit should converge to the step function. Our fitting function is given by

$$f(T) = A \tan^{-1}(\mathrm{B}(\mathrm{T} - \mathrm{T_c})) + \mathrm{D}, \tag{4.36}$$

where A, B, T_c and D are the fit parameters. If we choose $A = \frac{1}{\pi}$ and $D = 0.5$ and take the limit $B \to \infty$ then

$$\lim_{B\to\infty} \frac{1}{\pi} \tan^{-1}(\mathrm{B}(\mathrm{T} - \mathrm{T_c})) + 0.5 = \theta(\mathrm{T} - \mathrm{T_c}). \tag{4.37}$$

We see that it does converge to the required limit; so the function $f(T)$ is the correct choice. The values of fit parameters obtained after the fit are provided in Table 4.1. From this we conclude that the critical temperature $T_c = 1.068221 \pm 0.0173883$.

Internal Energy E and Extent of Space R^2

Figure 4.3 shows the plot of the scaled internal energy $\frac{E}{N^2}$ against temperature T. If we had simulated this for larger N then we would clearly see a kink near the critical temperature, which would directly show that the system undergoes a phase transition. But for smaller N this feature

Parameters	Fit Value	± error
A	0.288069	0.0107622
B	1.8178	0.123878
T_c	1.068221	0.0173883
D	0.509731	0.00582357

Table 4.1: Values of the fitting parameters A, B, T_c and D.

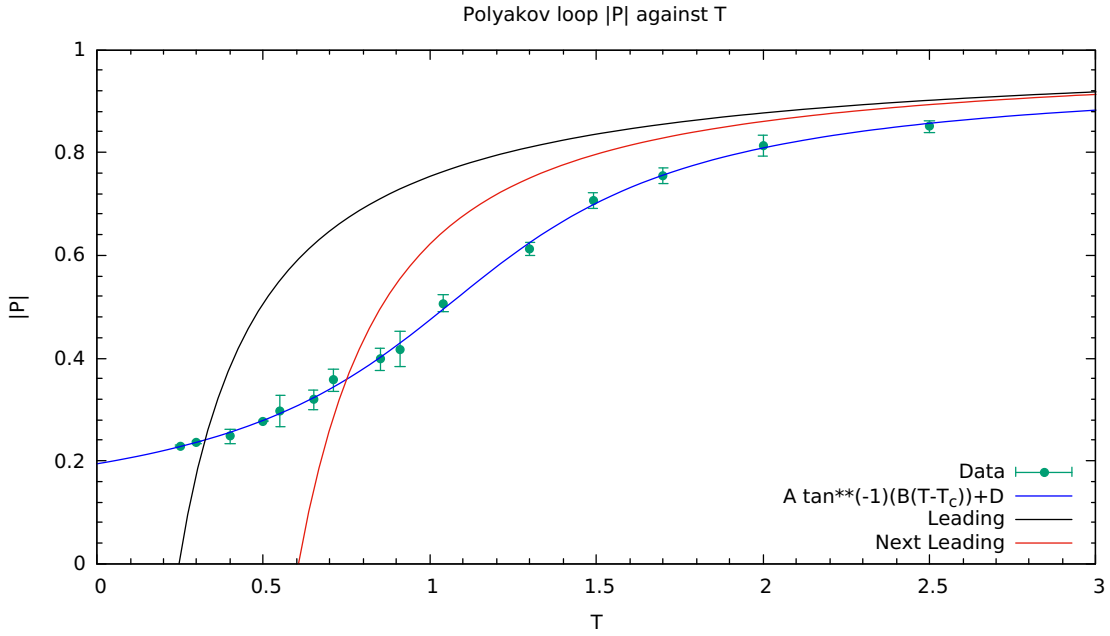

Figure 4.2: Polyakov loop against temperature T.

is not visible in the plot. The plot agrees well with the high temperature expansion (HTE). In Fig. 4.4 we show the plot of the extent of space R^2 against temp T.

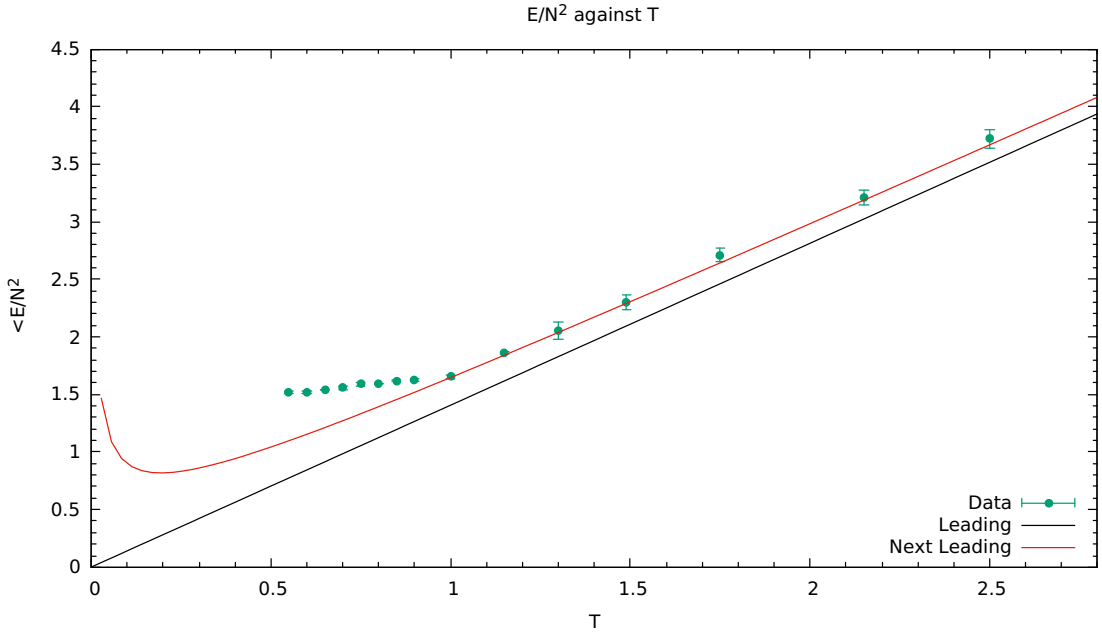

Figure 4.3: Plot of E/N^2 against temperature T.

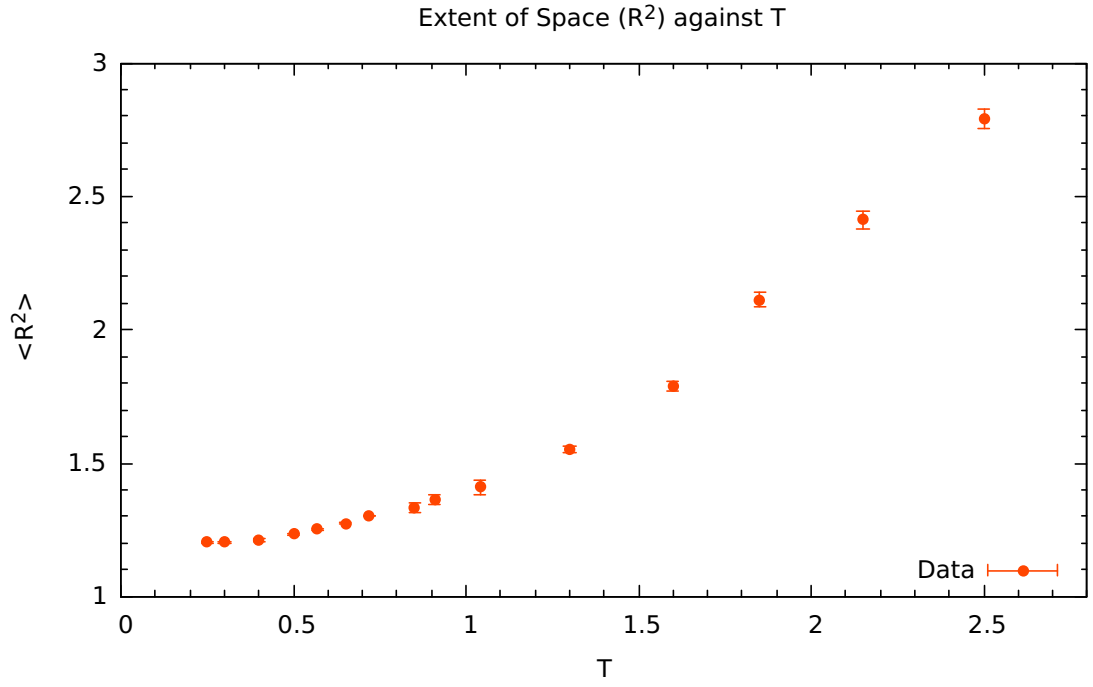

Figure 4.4: Plot of R^2 against temperature T.

Chapter 5

Supersymmetric Matrix Quantum Mechanics

This chapter discusses the numerical simulations of the supersymmetric matrix quantum mechanics model with four supercharges. In the previous chapter, we discussed the bosonic counterpart of the model. We will now add fermions to our theory and study the full model.

5.1 Model and Non-Lattice Discretization

The model can be obtained formally by dimensionally reducing $4d$ $\mathcal{N}=1$ U(N) super Yang-Mills theory to 1d, and it can be viewed as a one-dimensional U(N) gauge theory.

The Euclidean action of the full model is given by

$$S_E = \frac{1}{g^2}\int_0^\beta dt\ \ tr\Big[\frac{1}{2}(D_t X_i)^2 - \frac{1}{4}[X_i,X_j]^2 + \bar{\psi}D_t\psi - \bar{\psi}\sigma_i[X_i,\psi]\Big], \tag{5.1}$$

where $D_t X^i = \partial_t X^i - i[\ A(t), X^i(t)\ ]$, X_i are $N\times N$ Hermitian matrices; λ is the 't Hooft coupling; the fermionic matrices $\psi_\alpha(t)$ and $\bar{\psi}_\alpha(t)(\alpha=1,2)$ are $N\times N$ matrices with complex Grassmann entries. The 2×2 matrices σ_i are the Pauli matrices. Let us assume the boundary conditions to be periodic for bosons and anti-periodic for fermions. The extent β in the Euclidean time direction then corresponds to the inverse temperature $\beta \equiv 1/T$.

We use the following Fourier transformation equations

$$X_i^{ab}(t) = \sum_{n=-\Lambda}^{\Lambda} \tilde{X}_{in}^{ab} e^{i\omega nt}\ \ ;\ \ \psi_\alpha^{ab}(t) = \sum_{r=-\Lambda}^{\Lambda} \tilde{\psi}_{\alpha r}^{ab} e^{i\omega rt} \tag{5.2}$$

and similarly for $\bar{\psi}$, where r takes half-integer values, due to the anti-periodic boundary conditions, and $\lambda \equiv \Lambda - \frac{1}{2}$. Eq. (5.1) can then be written as

$$S_E = S_b + S_F \tag{5.3}$$

$$S_b = N\beta \left[\frac{1}{2} \sum_{n=-\Lambda}^{\Lambda} \left\{ n\omega - \frac{\alpha_a - \alpha_b}{\beta} \right\}^2 \tilde{X}^{ba}_{i,-n} \tilde{X}^{ab}_{in} - \frac{1}{4} \left([X_i, X_j]^2 \right)_0 \right] \tag{5.4}$$

$$S_f = N\beta \sum_{r=-\Lambda}^{\Lambda} \left[i \left\{ r\omega - \frac{\alpha_a - \alpha_b}{\beta} \right\} \tilde{\bar{\psi}}^{ba}_{\alpha r} \tilde{\psi}^{ab}_{\alpha r} - \underbrace{(\sigma_i)_{\alpha\beta} \mathrm{tr} \left\{ \tilde{\bar{\psi}}_{\alpha \mathrm{r}} \left([\tilde{\mathrm{X}}_{\mathrm{i}}, \tilde{\psi}_{\beta}] \right)_{\mathrm{r}} \right\}}_{\mathrm{M}} \right]. \tag{5.5}$$

The partition function of this model is given by

$$Z = \int \mathscr{D}X \;\; \mathscr{D}\psi \;\; \exp(-S_E). \tag{5.6}$$

We can integrate out the fermions from this partition function. For that, we first need to form the fermion matrix. We can simplify the fermionic part of the action to get the fermion matrix. First, we will decompose the fields with the help of the U(N) generators. We have

$$\tilde{X}_i = \sum_{C=1}^{N^2} \tilde{X}_i^C t^C, \;\; \tilde{\bar{\psi}}_{\alpha r} = \sum_{A=1}^{N^2} \tilde{\bar{\psi}}^A_{\alpha r} t^A, \;\; \tilde{\psi}_{\beta r} = \sum_{B=1}^{N^2} \tilde{\psi}^B_{\beta r} t^B, \tag{5.7}$$

where $\tilde{X}_i^C$ are real numbers, $\tilde{\psi}^A_{\beta r}$ and $\tilde{\bar{\psi}}^B_{\alpha r}$ are Grassmann numbers and the generators are normalized as $\mathrm{tr}(t_a t_b) = \delta_{ab}$.

Substituting this in the fermionic part of the action, we get

$$\begin{aligned}
M &= -N\beta(\sigma_i)_{\alpha\beta}\mathrm{Tr}\left\{\tilde{\bar{\psi}}_{\alpha \mathrm{r}}\left([\tilde{\mathrm{X}}_{\mathrm{i}},\tilde{\psi}_{\beta}]\right)_{\mathrm{r}}\right\} \\
&= -N\beta(\sigma_i)_{\alpha\beta}\mathrm{Tr}\left\{\tilde{\bar{\psi}}^{\mathrm{A}}_{\alpha \mathrm{r}}\mathrm{t}^{\mathrm{A}}\left([\tilde{\mathrm{X}}^{\mathrm{C}}_{\mathrm{i}}\mathrm{t}^{\mathrm{C}},\tilde{\psi}^{\mathrm{B}}_{\beta}\mathrm{t}^{\mathrm{B}}]\right)_{\mathrm{r}}\right\} \\
&= -N\beta(\sigma_i)_{\alpha\beta}\tilde{\bar{\psi}}^{A}_{\alpha r}\tilde{X}^{C}_{ir}\tilde{\psi}^{B}_{\beta r}\mathrm{Tr}\left(\mathrm{t}^{\mathrm{A}}[\mathrm{t}^{\mathrm{C}},\mathrm{t}^{\mathrm{B}}]\right) \\
&= -iN\beta(\sigma_i)_{\alpha\beta}\tilde{\bar{\psi}}^{A}_{\alpha r}\tilde{X}^{C}_{ir}\tilde{\psi}^{B}_{\beta r}f^{CBD}\mathrm{Tr}\left(\mathrm{t}^{\mathrm{A}}\mathrm{t}^{\mathrm{D}}\right) \quad (\mathrm{using}[\mathrm{t}^{\mathrm{C}},\mathrm{t}^{\mathrm{B}}] = \mathrm{i}\,\mathrm{f}^{\mathrm{CBD}}\mathrm{t}^{\mathrm{D}}) \\
&= -iN\beta(\sigma_i)_{\alpha\beta}\tilde{\bar{\psi}}^{A}_{\alpha r}\tilde{X}^{C}_{ir}\tilde{\psi}^{B}_{\beta r}f^{CBD}\delta_{AD} \qquad (\mathrm{usingtr}(\mathrm{t}^{\mathrm{A}}\mathrm{t}^{\mathrm{D}}) = \delta_{\mathrm{AD}}) \\
&= \tilde{\bar{\psi}}^{A}_{\alpha r}\left(iN\beta\sigma^{i}_{\alpha\beta}\tilde{X}^{C}_{ir}f^{ABC}\right)\tilde{\psi}^{B}_{\beta r}.
\end{aligned} \tag{5.8}$$

Finally, the fermionic action takes the form

$$S_F = N\beta\sum_{r=-\lambda}^{\lambda}\left[i\left\{r\omega - \frac{\alpha_a-\alpha_b}{\beta}\right\}\tilde{\bar{\psi}}^{A}_{\alpha r}(t^A)^{ba}\tilde{\psi}^{B}_{\alpha r}(t^B)^{ab} + \tilde{\bar{\psi}}^{A}_{\alpha r}\left(i(\sigma_i)_{\alpha\gamma}\tilde{X}^{C}_{ir}f^{ABC}\right)\tilde{\psi}^{B}_{\gamma r}\right]. \tag{5.9}$$

The fermionic action S_F may be written in the form $S_F = M_{A\alpha r;B\beta s}\tilde{\bar{\psi}}^{A}_{\alpha r}\tilde{\psi}^{B}_{\beta s}$. Here, the fermionic operator M is a $2(N^2)(2\lambda+1)\times 2(N^2)(2\lambda+1)$ size matrix with $A,B = 1,2,\cdots$, $\alpha,\beta = 1,2$ and r, s varies from $-\lambda$ to λ.

$$S_F = \sum_{A,B=1}^{N^2}\sum_{r,s=-\lambda}^{\lambda}\sum_{\alpha,\gamma=1}^{2}\tilde{\bar{\psi}}^{A}_{r\alpha}M_{A\alpha r,B\gamma s}\tilde{\psi}^{B}_{s\gamma}, \tag{5.10}$$

where

$$M_{A\alpha r,B\gamma s} = N\beta\left[i\left\{r\omega - \frac{\alpha_a-\alpha_b}{\beta}\right\}(t^A)^{ba}(t^B)^{ab}\delta_{\alpha\gamma}\delta_{rs} + \sigma^{i}_{\alpha\gamma}tr\left(\tilde{X}_{ir}[t^A,t^B]\right)\delta_{rs}\right]. \tag{5.11}$$

Now using the result that

$$\int d\psi\ \exp(-\psi^{\mathrm{T}}\mathrm{A}\psi) = \mathrm{Pf}(\mathrm{A}) = \det(\mathrm{A})^{1/2}\ \text{ where A is an antisymmetric matrix}$$

we can integrate out the fermions from the partition function Eq. (5.6). Integrating out the

fermions from the partition function we get

$$Z = \int \mathscr{D}X \;\; \exp\{-\mathrm{S_b}\}\mathrm{Pf(M)}, \tag{5.12}$$

where S_b is the bosonic part of the action. $Pf(M)$ for this model is a real number because the fermion determinant is real positive. One can then use the standard RHMC (Rational Hybrid Monte Carlo) or real Langevin method. We have used the real Langevin method for producing the results.

5.2 CLM for SUSY Model

We calculated the drift terms for the bosonic half in the previous chapter, and now we just need to include the contribution from the fermionic part.

The gradients of the fermionic operator can be computed using Eq. (5.11), and are given by

$$\frac{\partial M_{A\alpha r;B\gamma s}}{\partial(\tilde{X}_{ir})_{ba}} = N\beta\sigma^i_{\alpha\gamma}\left([t^A,t^B]\right)_{ab}, \tag{5.13}$$

$$\frac{\partial M_{A\alpha r;B\gamma r}}{\partial(\alpha_a)} = N(-i)\delta_{\alpha\gamma}\delta_{AB}. \tag{5.14}$$

The derivative identity of the Pfaffian states that if A relies on some variable x_i, then the Pfaffian's gradient can be manipulated as

$$\frac{1}{Pf(A)}\frac{\partial Pf(A)}{\partial x_i} = \frac{1}{2}\mathrm{tr}\left(\mathrm{A}^{-1}\frac{\partial \mathrm{A}}{\partial \mathrm{x_i}}\right). \tag{5.15}$$

Using Eq. (5.15), the final drift terms to be used in the Langevin equations can be written as

$$\frac{\partial S_{eff}}{\partial(\tilde{X}_{ir})_{ba}} = \frac{\partial S_B}{\partial(\tilde{X}_{ir})_{ba}} - \mathrm{tr}\left(\mathscr{M}^{-1}\frac{\partial \mathrm{M_{A\alpha r;B\gamma r}}}{\partial(\tilde{\mathrm{X}}_{\mathrm{ir}})_{\mathrm{ba}}}\right), \tag{5.16}$$

$$\frac{\partial S_{eff}}{\partial(\alpha_a)} = \frac{\partial S_B}{\partial(\tilde{X}_{ir})_{ba}} - \mathrm{tr}\left(\mathscr{M}^{-1}\frac{\partial \mathrm{M_{A\alpha r;B\gamma r}}}{\partial(\alpha_{\mathrm{a}})}\right). \tag{5.17}$$

Here we included the contribution from Faddeev-Popov term into the bosonic gradient.

5.3 Observables

The observable we are interested in is the Polyakov loop $|P|$. The definition and the discretized form is given below

- Polyakov loop $|P|$

$$\langle |P| \rangle \equiv \frac{1}{N} \left\langle \left| \mathscr{P}(e^{i \oint dt A(t)}) \right| \right\rangle = \left\langle \left| \frac{Tr(U)}{N} \right| \right\rangle, \tag{5.18}$$

  where the symbol $\mathscr{P}$ exp represents the path-ordered exponential and the unitary matrix U is called the holonomy matrix.

5.4 Simulation Details and Results

The simulations were performed for $N = 2$ and $\Lambda = 4$. All other simulation parameters are same as used for the bosonic model.

Figure (5.1) show the results for the Polyakov line, for the bosonic and supersymmetric cases.

For the supersymmetric case, our preliminary results with $\Lambda = 4$ reproduce the asymptotic behavior at large T obtained by the high temperature expansion (HTE) [Kawahara 07b] up to the next-leading order. (The solid lines represent the results at the leading order of HTE, which are the same for the bosonic and SUSY cases.) Note that the non-lattice method is applicable also at low temperature, where the HTE is no longer valid.

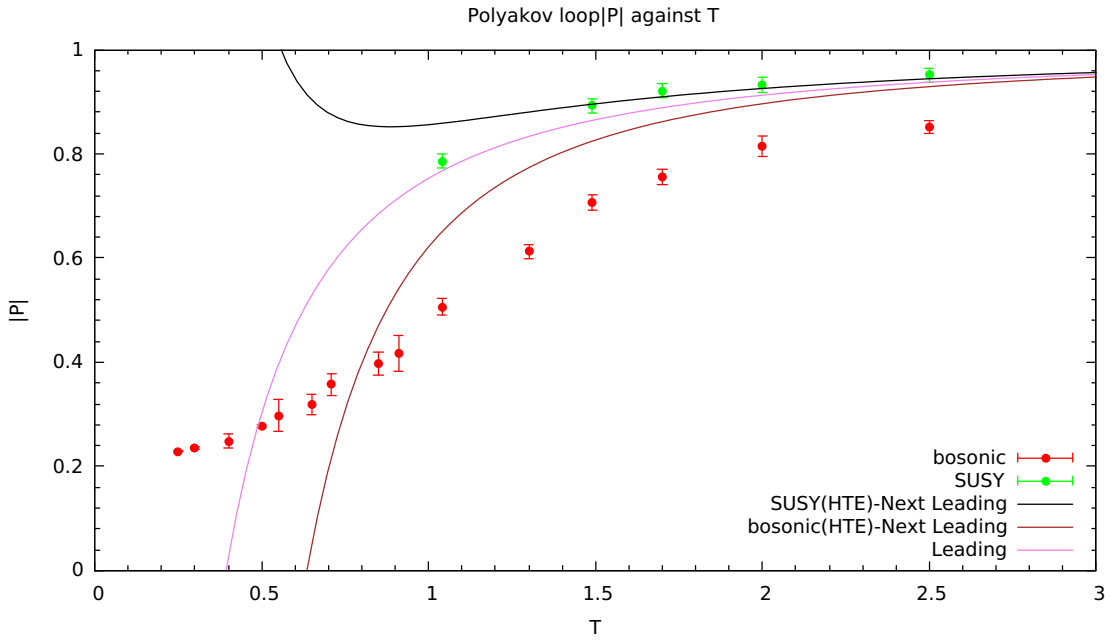

Figure 5.1: Polyakov loop against temperature T.

Chapter 6

Summary and Concluding Remarks

The goal of this thesis is to explore the non-lattice approach and apply the method to several supersymmetric models. We used complex Langevin method for simulations.

In the bosonic matrix quantum mechanics case, we used Polyakov loop as an order parameter to investigate the phase structure of the model at finite temperature. We clearly observed the confinement-deconfinement phase transition. From the energy vs temperature plot it is clear that the phase transition is of second order. All our results are consistent with the results produced by other authors.

In the SUSY MQM case, our preliminary results reproduce the asymptotic behavior at large T obtained by the high temperature expansion up to the next-leading order.

The perk of using non-lattice method is that Fourier acceleration requires no extra cost, since we deal with the Fourier modes directly. The continuum limit is achieved much faster than one would expect naively from the number of degrees of freedom. This is understandable since the Fourier modes omitted by the cutoff scheme are naturally suppressed by the kinetic term.

It is simple to apply the non-lattice method to the case of sixteen supercharges, which is more interesting due to its dual relationship with type IIA supergravity theory. In the future, we can use complex Langevin or Monte Carlo simulations to investigate the sixteen supercharge model. This study has been discussed in the Ref. [Anagnostopoulos 08].

Appendix A

Noisy Estimator for Tr $\left(\frac{\partial M}{\partial \tilde{\phi}_n} M^{-1}\right)$.

In the simulations of Chapter 3, we did not use a noisy estimator, since calculating M^{-1} does not take much CPU cost. For the trace of the general $m \times m$ matrix M, we prepare a white-noise vector $\eta_i (i = 1, 2, \cdots, m)$ obeying $\langle \eta_i^* \eta_j \rangle = \delta_{ij}$. To that end, we set

$$\eta_j = \frac{X_j + iY_j}{\sqrt{2}}, \quad \eta_j^* = \frac{X_j - iY_j}{\sqrt{2}}, \quad \mathrm{where X_j, Y_j obey N}(0,1). \tag{A.1}$$

In this case, we have

$$\langle \eta_j^* \eta_j \rangle = \frac{1}{2}\{\langle X_j^2 \rangle + \langle Y_j^2 \rangle\} = 1, \quad \langle \eta_i^* \eta_j \rangle = 0 (i \neq j). \tag{A.2}$$

Then, we have

$$\sum_{j,k=1}^{m} \langle \eta_j^* M_{jk} \eta_k \rangle = \sum_{j,k=1}^{m} M_{jk} \langle \eta_j^* \eta_k \rangle = \sum_{j,k=1}^{m} M_{jk} \delta_{jk} = \sum_{k=1}^{m} M_{kk} = \mathrm{Tr} M. \tag{A.3}$$

In the present case, we prepare a noise vector η_{k_i} $(k_i = -\Lambda, \cdots, \Lambda)$ obeying

$$\langle \eta_{k_1}^* \eta_{k_2} \rangle = \delta_{k_1 k_2}. \tag{A.4}$$

Then, the trace is estimated as (here, we omit the Langevin time (n)).

$$\mathrm{Tr}\left(\frac{\partial M}{\partial \tilde{\phi}_n} M^{-1}\right) = \left\langle \eta^* \frac{\partial M}{\partial \tilde{\phi}_n} \underbrace{M^{-1} \eta}_{=X} \right\rangle = \left\langle \eta_{k_1}^* \left(\frac{\partial M}{\partial \tilde{\phi}_n}\right)_{k1k2} X_{k_2} \right\rangle \tag{A.5}$$

$X = M^{-1}\eta$ can be calculated via the conjugate gradient (CG) method. It is convenient to solve

$$M^\dagger M X = M^\dagger \eta \tag{A.6}$$

since the CG method is applicable to a *symmetric and positive-definite matrix*. Also, we comment that in Langevin simulation we do not need to take the average of $\left\langle \eta^* \frac{\partial M}{\partial \tilde{\phi}_n} \underbrace{M^{-1}\eta}_{=X} \right\rangle$. Just one noisy estimator is enough, since the Fokker-Planck equation will be the same as the one we obtain when we treat Tr $\left(\frac{\partial M}{\partial \tilde{\phi}_n} M^{-1}\right)$ exactly.

Appendix B

Derivation of a Formula for the Internal Energy

In this section, we derive the formula Eq. (4.31) that relates the internal energy of the current model to the expected value Eq. (4.32), which is directly accessible through Monte Carlo simulation.

Let us simplify Eq. (4.30)

$$E = -\frac{1}{Z(\beta)} \lim_{\Delta\beta \to 0} \frac{Z(\beta') - Z(\beta)}{\Delta\beta}. \tag{B.1}$$

Here $\beta' = \beta + \Delta\beta$, and represent $Z(\beta')$ for later convenience as

$$Z(\beta') = \int [\mathscr{X}'_{beta'}][\mathscr{A}']_{\beta'} e^{-S'}, \tag{B.2}$$

where S' is deduced from S given in Eq. (4.9) by substituting $\beta, t, A(t), X_i(t)$ with $\beta', t', A'(t'), X_i'(t')$.

In order to connect $Z(\beta')$ with $Z(\beta)$, we consider the transformation

$$t' = \frac{\beta'}{\beta} t, \;\; A'(t') = \frac{\beta}{\beta'} A(t), \;\; X_i'(t') = \sqrt{\frac{\beta'}{\beta}} X_i(t). \tag{B.3}$$

The factors in front of the fields are inspired on the basis of dimensions, and we have in particular we have $[\mathscr{D}X']_{\beta'} = [\mathscr{D}X]_{\beta}$ and $[\mathscr{D}A']_{\beta'} = [\mathscr{D}A]_{\beta}$. The kinetic term in S' is reduced to that in S by this transformation, but the interaction term transforms non-trivially as

$$\int_0^{\beta'} dt' tr\left([X_i'(t'), X_j'(t')]^2\right) = \left(\frac{\beta'}{\beta}\right)^3 \int_0^{\beta} \mathrm{dt\ tr}\left([\mathrm{X_i(t)}, \mathrm{X_j(t)}]^2\right). \tag{B.4}$$

This gives us the relation

$$Z(\beta') = Z(\beta)\left\{1 - \frac{3}{4}N^2\Delta\beta\langle F^2\rangle + O\left((\Delta\beta)^2\right)\right\}, \tag{B.5}$$

where the operator F^2 is defined by Eq. (4.32). Plugging this into Eq. (B.1) we get Eq. (2.8).

Bibliography

[Aarts 10a] Gert Aarts, Frank A. James, Erhard Seiler & Ion-Olimpiu Stamatescu. *Adaptive step size and instabilities in complex Langevin dynamics*. Physics Letters B, vol. 687, no. 2-3, pages 154–159, apr 2010.

[Aarts 10b] Gert Aarts, Erhard Seiler & Ion-Olimpiu Stamatescu. *Complex Langevin method: When can it be trusted?* Physical Review D, vol. 81, no. 5, mar 2010.

[Aarts 11a] Gert Aarts, Frank A. James, Erhard Seiler & Ion-Olimpiu Stamatescu. *Complex Langevin dynamics: criteria for correctness*, 2011.

[Aarts 11b] Gert Aarts, Frank A. James, Erhard Seiler & Ion-Olimpiu Stamatescu. *Complex Langevin: etiology and diagnostics of its main problem*. The European Physical Journal C, vol. 71, no. 10, oct 2011.

[Aarts 13a] Gert Aarts, Lorenzo Bongiovanni, Erhard Seiler, Dénes Sexty & Ion-Olimpiu Stamatescu. *Controlling complex Langevin dynamics at finite density*. The European Physical Journal A, vol. 49, no. 7, jul 2013.

[Aarts 13b] Gert Aarts, Pietro Giudice & Erhard Seiler. *Localised distributions and criteria for correctness in complex Langevin dynamics*. Annals of Physics, vol. 337, pages 238–260, oct 2013.

[Aarts 13c] Gert Aarts, Frank A. James, Jan M. Pawlowski, Erhard Seiler, Dénes Sexty & Ion-Olimpiu Stamatescu. *Stability of complex Langevin dynamics in effective models*. Journal of High Energy Physics, vol. 2013, no. 3, mar 2013.

[Aharon 04] Ofer Aharon, Joseph Marsano, Shiraz Minwalla & Toby Wiseman. *Black hole black string phase transitions in thermal (1 + 1)-dimensional supersymmetric Yang-Mills theory on a circle*. Classical and Quantum Gravity, vol. 21, no. 22, pages 5169–5191, oct 2004.

[Ambjorn 86] Jan Ambjorn, M. Flensburg & C. Peterson. *The Complex Langevin Equation and Monte Carlo Simulations of Actions With Static Charges*. Nucl. Phys. B, vol. 275, pages 375–397, 1986.

[Ambjørn 00] Jan Ambjørn, Jun Nishimura, Konstantinos N Anagnostopoulos, Wolfgang Bietenholz & Tomohiro Hotta. *Large N dynamics of dimensionally reduced 4D SU(N) super Yang-Mills theory*. Journal of High Energy Physics, vol. 2000, no. 07, pages 013–013, jul 2000.

[Anagnostopoulos 08] Konstantinos N. Anagnostopoulos, Masanori Hanada, Jun Nishimura & Shingo Takeuchi. *Monte Carlo Studies of Supersymmetric Matrix Quantum Mechanics with Sixteen Supercharges at Finite Temperature*. Physical Review Letters, vol. 100, no. 2, jan 2008.

[Banks 97] T. Banks, W. Fischler, S. H. Shenker & L. Susskind. *M-theory as a matrix model: A conjecture*. Physical Review D, vol. 55, no. 8, page 5112–5128, Apr 1997.

[Bergner 08] G. Bergner, T. Kaestner, S. Uhlmann & A. Wipf. *Low-dimensional supersymmetric lattice models*. Annals of Physics, vol. 323, no. 4, pages 946–988, apr 2008.

[Damgaard 87] Poul H. Damgaard & Helmuth Huffel. *Stochastic Quantization*. Phys. Rept., vol. 152, page 227, 1987.

[Drell 76] Sidney D. Drell, Marvin Weinstein & Shimon Yankielowicz. *Strong-coupling field theories. II. Fermions and gauge fields on a lattice*. Phys. Rev. D, vol. 14, pages 1627–1647, Sep 1976.

[Furuuchi 03] K. Furuuchi, E. Schreiber & G. W. Semenoff. *Five-Brane Thermodynamics from the Matrix Model*, 2003.

[Gausterer 88] H. Gausterer & S. Sanielevici. *Remarks on the Numerical Solution of Langevin Equations on Unitary Group Spaces*. Comput. Phys. Commun., vol. 52, pages 43–48, 1988.

[Giedt 06] Joel Giedt. *Advances and applications of lattice supersymmetry*. PoS, vol. LAT2006, page 008, 2006.

[Hadizadeh 05] Shirin Hadizadeh, Bojan Ramadanovic, Gordon W. Semenoff & Donovan Young. *Free energy and phase transition of the matrix model on a plane wave*. Physical Review D, vol. 71, no. 6, mar 2005.

[Hanada 07] Masanori Hanada, Jun Nishimura & Shingo Takeuchi. *Non-lattice simulation for supersymmetric gauge theories in one dimension*. Phys. Rev. Lett., vol. 99, page 161602, 2007.

[Ishii 08] Takaaki Ishii, Goro Ishiki, Shinji Shimasaki & Asato Tsuchiya. $\mathcal{N} = 4$ *super Yang-Mills theory from the plane wave matrix model*. Physical Review D, vol. 78, no. 10, nov 2008.

[Ishiki 09] Goro Ishiki, Sang-Woo Kim, Jun Nishimura & Asato Tsuchiya. *Deconfinement phase transition in* $\mathcal{N} = 4$ *super Yang-Mills theory on* $R \times S^3$ *from supersymmetric matrix quantum mechanics*. Phys. Rev. Lett., vol. 102, page 111601, 2009.

[Itzhaki 98] Nissan Itzhaki, Juan M. Maldacena, Jacob Sonnenschein & Shimon Yankielowicz. *Supergravity and The Large N Limit of Theories With Sixteen Supercharges*. Physical Review D, vol. 58, no. 4, jul 1998.

[Janik 00] R. A. Janik & J. Wosiek. *Towards the matrix model of M-theory on a lattice*. 2000.

[Kaplan 05] David B Kaplan & Mithat Ünsal. *A euclidean lattice construction of supersymmetric Yang-Mills theories with sixteen supercharges*. Journal of High Energy Physics, vol. 2005, no. 09, pages 042–042, sep 2005.

[Kawahara 05] Naoyuki Kawahara & Jun Nishimura. *The large-N reduction in matrix quantum mechanics — a bridge between BFSS and IKKT*. Journal of High Energy Physics, vol. 2005, no. 09, page 040–040, Sep 2005.

[Kawahara 07a] Naoyuki Kawahara, Jun Nishimura & Shingo Takeuchi. *Exact fuzzy sphere thermodynamics in matrix quantum mechanics*. Journal of High Energy Physics, vol. 2007, no. 05, page 091–091, May 2007.

[Kawahara 07b] Naoyuki Kawahara, Jun Nishimura & Shingo Takeuchi. *High temperature expansion in supersymmetric matrix quantum mechanics*. Journal of High Energy Physics, vol. 2007, no. 12, pages 103–103, dec 2007.

[Klauder 85a] John R. Klauder & Wesley P. Petersen. *Spectrum of certain non-self-adjoint operators and solutions of Langevin equations with complex drift*. Journal of Statistical Physics, vol. 39, no. 1-2, pages 53–72, April 1985.

[Klauder 85b] John R Klauder & Wesley P Petersen. *Spectrum of certain non-self-adjoint operators and solutions of Langevin equations with complex drift*. Journal of statistical physics, vol. 39, no. 1, pages 53–72, 1985.

[Lemons 97] Don Lemons & Anthony Gythiel. *Paul Langevin's 1908 paper "On the Theory of Brownian Motion"*. American Journal of Physics - AMER J PHYS, vol. 65, pages 1079–1081, 01 1997.

[Mathur 08] Samir D. Mathur. *Fuzzballs and the information paradox: a summary and conjectures*, 2008.

[Nagata 16] Keitaro Nagata, Jun Nishimura & Shinji Shimasaki. *Argument for justification of the complex Langevin method and the condition for correct convergence*. Physical Review D, vol. 94, no. 11, dec 2016.

[Parisi 81] G. Parisi & Yong-shi Wu. *Perturbation Theory Without Gauge Fixing*. Sci. Sin., vol. 24, page 483, 1981.

[Polyakov 78] Alexander M. Polyakov. *Thermal properties of gauge fields and quark liberation*. Physics Letters, Section B: Nuclear, Elementary Particle and High-Energy Physics, vol. 72, no. 4, pages 477–480, January 1978.

[Semenoff] Gordon W. Semenoff. Matrix model thermodynamics, pages 601–613.